Morphological and genetic diversity of Beaufort Sea diatoms with high contributions from the *Chaetoceros neogracilis* species complex

Balzano Sergio [1, *], Percopo Isabella [2], Siano Raffaele [3], Gourvil Priscillia [4], Chanoine Mélanie [4], Dominique Marie [4], Vaulot Daniel [4], Sarno Diana [5]

[1] Sorbonne Universités, UPMC Univ Paris 06, CNRS, UMR7144, Station Biologique De Roscoff; 29680 Roscoff, France
[2] Integrative Marine Ecology Department, Stazione Zoologica Anton Dohrn; Villa Comunale 80121 Naples ,Italy
[3] IFREMER, Dyneco Pelagos; Bp 70 29280 Plouzane ,France
[4] Sorbonne Universités, UPMC Univ Paris 06, CNRS, UMR7144, Station Biologique de Roscoff; 29680 Roscoff ,France
[5] Integrative Marine Ecology Department; Stazione Zoologica Anton Dohrn; Villa Comunale 80121 Naples, Italy

* Corresponding author : Sergio Balzano, email address : Sergio.Balzano@nioz.nl

Abstract :

Seventy-five diatoms strains isolated from the Beaufort Sea (Canadian Arctic) in the summer of 2009 were characterized by light and electron microscopy (SEM and TEM) as well as 18S and 28S rRNA gene sequencing. These strains group into 20 genotypes and 17 morphotypes and are affiliated with the genera *Arcocellulus*, *Attheya*, *Chaetoceros*, *Cylindrotheca*, *Eucampia*, *Nitzschia*, *Porosira*, *Pseudo-nitzschia*, *Shionodiscus*, *Thalassiosira*, *Synedropsis*. Most of the species have a distribution confined to the northern/polar area. *Chaetoceros neogracilis* and *Chaetoceros gelidus* were the most represented taxa. Strains of *C. neogracilis* were morphologically similar and shared identical 18S rRNA gene sequences, but belonged to four distinct genetic clades based on 28S rRNA, ITS-1 and ITS-2 phylogenies. Secondary structure prediction revealed that these four clades differ in hemi-compensatory base changes (HCBCs) in paired positions of the ITS-2, suggesting their inability to interbreed. Reproductively isolated *C. neogracilis* genotypes can thus co-occur in summer phytoplankton communities in the Beaufort Sea. *Chaetoceros neogracilis* generally occurred as single cells but can also form short colonies. It is phylogenetically distinct from an Antarctic species, erroneously identified in some previous studies as *C. neogracilis* but named here as *Chaetoceros* sp. This work provides taxonomically validated sequences for 20 Arctic diatom taxa, which will facilitate future metabarcoding studies on phytoplankton in this region.

Keywords : biogeography, ITS, ITS2 secondary structure, LSU, morphology, phylogeny, polar diatoms, SSU

INTRODUCTION

Due to fluctuations in light, temperature, salinity and sea ice extent, Arctic phytoplankton undergo high seasonal variability in abundance and composition. Higher temperatures and longer daylight between March and September, lead to an increase in algal biomass and primary production (Sherr et al. 2003, Wang et al. 2005). Diatoms account for a high portion of Arctic phytoplankton, especially in coastal locations (Booth & Horner 1997, Lovejoy et al. 2002) and species belonging to the genera *Chaetoceros* Ehrenberg and *Thalassiosira* Cleve can dominate phytoplankton communities in different regions (Tuschling et al. 2000, Booth et al. 2002, Ratkova & Wassmann 2002).

The Beaufort Sea is a major component of the Arctic Ocean, and is highly influenced by the Mackenzie River, which plays a key role in disrupting the winter ice in early spring promoting primary production and phytoplankton blooms (Carmack & MacDonald 2002). In addition, periodic wind-driven upwelling events can bring nutrient rich waters up to the surface layer and promote phytoplankton growth (Pickart et al. 2013). Except during episodic upwelling events,

the water column is highly stratified, the nutrient concentration in the upper layers is extremely low, leading to the prevalence of picoeukaryotes, mostly represented by the psychrophilic *Micromonas* Manton & Parke ecotype corresponding to the single genetic clade named "Arctic *Micromonas*" (Lovejoy et al. 2007, Balzano et al. 2012b), within the phytoplankton community. Diatoms tend to be more abundant near the coast (Hill et al. 2005), occasionally blooming in late spring (Hill et al. 2005, Sukhanova et al. 2009). The algal biomass and the contribution of diatoms to the phytoplankton community increase in summer (Hill et al. 2005) and diatoms bloom more frequently at the deep chlorophyll maximum (DCM; Sukhanova et al. 2009). Autumn communities include higher contributions of dinoflagellates, which can dominate the community along with diatoms (Brugel et al. 2009).

The MALINA oceanographic expedition sailed in July 2009 from the Pacific coast of Canada to the Beaufort Sea where an extensive multidisciplinary sampling effort was undertaken until mid-August. Pigment analyses (Coupel et al. 2015) and light microscopy techniques (http://malina.obs-vlfr.fr/data.html) confirmed previous findings on phytoplankton community composition and revealed that Prymnesiophyceae, Mamiellophyceae and Dinophyceae dominated offshore waters while diatoms accounted for most abundance and biomass on the Mackenzie Shelf (Coupel et al. 2015). Within diatoms the cold-water ecotype of *Chaetoceros socialis* described recently as *Chaetoceros gelidus* (Degerlund et al. 2012, Chamnansinp et al. 2013), several other *Chaetoceros* taxa, and with lower abundances, *Thalassiosira nordenskioeldii,* and *Pseudo-nitzschia* spp. prevailed (http://malina.obs-vlfr.fr/data.html). Molecular techniques [cloning/sequencing and terminal-RFLP (T-RFLP) on the 18S rRNA gene] on photosynthetic populations (Balzano et al. 2012b) partially agree with pigment analyses and

phytoplankton microscopy counts indicating that Arctic *Micromonas* (Lovejoy et al. 2007) was the only photosynthetic picoplankter (< 2 μm) detected in most stations, whereas nanoplankton (2-20 μm) genetic libraries were dominated by the diatoms *C. gelidus* (referred therein as *C. socialis*) and *Chaetoceros neogracilis* in DCM and surface waters, respectively (Balzano et al. 2012b).

Seasonal succession and geographic distribution of phytoplankton species have thus been partially elucidated for the Beaufort Sea, but species level diversity has still not been fully assessed for diatoms, due to the limited resolution power of the morphological and molecular methods employed. Light microscopy, that has been applied in most the studies, does not allow the observation of the fine ultrastructural details often required to distinguish diatom species. Similarly, the 18S rRNA gene did not allow discrimination among some species of the genera *Chaetoceros* and *Pseudo-nitzschia* H. Peragallo, which were well represented in the area (Balzano et al. 2012b). Other ribosomal genes have a higher resolution power: the 28S rRNA gene can successfully discriminate most of the species within the genera *Chaetoceros* (Kooistra et al. 2010) and *Pseudo-nitzschia* (Lundholm et al. 2002) and is considered a good discriminatory molecular marker among centric diatom species (Lee et al. 2013). A gene fragment extending from the 5$^{'}$ end of the 5.8S to the 3' end of the helix III of ITS-2 (5.8S + ITS-2) has been proved to separate the 99.5 % of diatom species (Moniz & Kaczmarska 2010).

Coupling culture isolation with morphological and genetic characterization allows detailed species identification. This approach has been applied to photosynthetic flagellates collected during the MALINA cruise. Photosynthetic pico- and nanoeukaryotic populations were

dominated by cultured microorganisms (Balzano et al. 2012b) and 104 strains belonging to the Chlorophyta, Dinophyta, Haptophyta, Cryptophyta and Heterokontophyta divisions were isolated and characterized by both light microscopy (LM) and 18S rRNA gene sequencing (Balzano et al. 2012a).

A recent study investigated Arctic dinoflagellates coupling morphological and genetic approaches (Gu et al. 2013), but similar information on diatoms is missing. In the present paper, we focus on diatom strains isolated from the Beaufort Sea. We combined LM, TEM, and SEM with 18S and 28S rRNA gene sequencing to identify the isolated strains. We also sequenced the ITS operon of the rRNA gene from a number of *C. neogracilis* strains sharing highly similar 18S and 28S rRNA gene sequences to further investigate the occurrence of distinct genetic entities and we reconstructed the secondary structure of the ITS-2 of these strains in order to predict their reproductive isolation.

MATERIALS AND METHODS

Phytoplankton sampling, isolation and maintenance. Strains were isolated from seawater samples collected during the MALINA (http://www.obs-vlfr.fr/Malina) cruise which sailed the 06/07/09 from Victoria (British Columbia, Canada) to the Beaufort Sea where an extensive sampling effort was carried out in late summer from 1/08/09 to 24/08/09 (Table S1 in the Supporting Information). Samples were collected with a bucket from surface waters in the North Pacific and at different depths with Niskin bottles mounted on a CTD frame in the Beaufort Sea. Phytoplankton strains were isolated both onboard and back in the laboratory (Table 1) as described previously (Le Gall et al. 2008, Balzano et al. 2012a). Overall we isolated 75 diatom strains, 60 of which are currently (March 2016) available from the Roscoff Culture Collection

(RCC: http://www.roscoff-culture-collection.org/). Most of the strains were isolated from the Beaufort Sea but we also included four strains from the North Pacific sampled during the first leg of the MALINA cruise for comparison purposes. The strains were maintained in K or K/2-medium (Keller et al. 2009) with addition of silicate, prepared from sterile seawater at a salinity of 35 and kept at 4°C at an irradiance of 50 µmol photons $\cdot$ m^{-2} $\cdot$ s^{-1} in a 12:12 light dark regime. Some of the *C. neogracilis* strains were incubated at low light intensity (about 10 µmol photons $\cdot$ m^{-2} $\cdot$ s^{-1}) in f/2 medium (Guillard 1975) with nitrate supplied at a concentration 10-fold lower (88 µM) to induce resting spore formation, since spore morphology can help species identification in the genus *Chaetoceros* (Hasle & Syvertsen 1997).

DNA extraction and PCR. Genomic DNA was extracted from 75 MALINA strains as described previously (Balzano et al. 2012a) using the NucleoSpin Tissue kit (Mackerey Nagel, Hoerdt, France) and following the instructions provided by the manufacturer.

The 18S rRNA gene, the Internal Transcribed Spacer (ITS) of the rRNA operon and the 28S rRNA gene were then amplified by PCR on genomic DNA. For the 18S rRNA gene the primers 63f (5'-ACGCTT-GTC-TCA-AAG-ATTA-3') and 1818r (5'-ACG-GAAACC-TTG-TTA-CGA-3') were used (Lepère et al. 2011) as described previously (Balzano et al. 2012a).

The ITS region of the rRNA operon was amplified from 35 MALINA strains of *C. neogracilis* (Table 1) and 3 Antarctic strains of *Chaetoceros* purchased from the National Centre for Marine Algae and Microbiota (Bigelow, USA) and previously thought to belong to *C. neogracilis* (CCMP187, CCMP189, and CCMP190; Table S2 in the Supporting Information).

The ITS was amplified using primers 329f (5'-GTG-AAC-CTG-CRG-AAG-GAT-CA-3') and D1R-R (5'- TAT-GCT-TAA-ATT-CAG-CGG-GT-3') which correspond to the reverse complements of the reverse primer for 18S 329r (Guillou et al. 2004) and the 28S forward primer D1R (Lenaers et al. 1989), respectively. PCR condition included an initial incubation step at 95°C during 5 min, 35 amplification cycles (95°C for 1 min, 55°C for 45 s, and 72°C for 1 min 15 s) and a final elongation step at 72 °C for 7 min. From 72 diatom strains, the 28S rRNA gene was amplified using primers D1R (5'-ACC-CGC-TGA-ATT-TAA-GCA-TA-3') and D3Ca (5'-ACG-AAC-GAT-TTG-CAC-GTC-AG-3') targeting the D1–D3 region of the nuclear LSU rRNA (Lenaers et al. 1989, Orsini et al. 2002). PCR reactions were as follows: 30 amplification cycles of 94°C for 1 min, 55°C for 1 min 30 s, and 72°C for 1 min.

18S rRNA, ITS, and 28S rRNA amplicons were purified using Exosap (USB products, Santa Clara, USA) and partial sequences were determined by using Big Dye Terminator V3.1 (Applied Biosystems, Foster city, USA). The hypervariable V4 region (Dunthorn et al. 2012) of the 18S rRNA gene was sequenced from all the strains using the internal primer Euk528f (Zhu et al. 2005), whereas the primers 63f and 1818R were used to sequence the full 18S rRNA gene from selected strains. The ITS region was sequenced using both forward and reverse primers described above whereas the forward primer D1R was used to sequence the 28S rRNA gene. Sequencing was carried out on an ABI prism 3100 sequencer (Applied Biosystems).

Phylogenetic analysis.   V4 sequences were compared to those available in Genbank using BLAST (blast.ncbi.nlm.nih.gov/Blast.cgi), aligned using ClustalW2 (http://www.ebi.ac.uk/Tools/msa/clustalw2) and then grouped into 17 different 18S genotypes based on 99.5% sequences similarity, using the Bioedit software (Hall 1999). The full 18S rRNA

gene was sequenced from at least one strain per genotype (19 strains in total). For all the phylogenetic trees shown in this paper, relationships were analyzed using Maximum Likelihood (ML) and Neighbour Joining (NJ) methods (Nei & Kumar 2000) and bootstrap values were estimated using 1,000 replicates (Felsenstein 1985) for both methods. MEGA5 software (Tamura et al. 2011) was used to construct the phylogenetic trees based on the ML topology.

Full 18S rRNA sequences were aligned with reference sequences from Genbank (http://www.ncbi.nlm.nih.gov/nucleotide, Table S2) for a total of 84 sequences using clustalW2 as described above. Highly variable regions of the alignment were removed and the final dataset contained 1,465 nucleotide positions. A Tamura Nei model (Tamura & Nei 1993) was selected as the best model to infer both NJ and ML 18S phylogeny.

For the D1-D3 region of the 28S rRNA gene 64 sequences were aligned using clustalw2 and a subset, containing at least one sequence per genotype, was used to construct three phylogenetic trees (centric diatoms, pennate diatoms and *C. neogracilis* strains). Highly variable regions were removed from the alignments. For the centric diatoms, the alignment included, 65 sequences and 504 positions and the phylogeny was inferred using a Kimura-2 model (Kimura 1980). Phylogenetic relationships were then inferred as described above and 5 sequences from the genus *Attheya* West were used as an outgroup and were then removed from the tree for clarity. For the pennate diatoms, the alignment included 35 sequences and 490 nucleotide positions and the phylogeny was inferred using a Tamura-Nei model (Tamura & Nei 1993) and sequences from the genus *Attheya* were also used as an outgroup. A third phylogenetic tree was constructed for *C. neogracilis*, which included 36 MALINA strains from this species, 1 sequence of the strain

CPH9 identified as *Chaetoceros fallax* Prosckina Lavrenko, 3 GenBank sequences from the

Antarctic strains CCMP163, CCMP189 and CCMP190 (Table S2) and one sequence from *C.*

gelidus (RCC2271) which was used as an outgroup. The analysis was performed on 41

sequences for a total of 590 positions using a Kimura-2-parameter model.

We also sequenced the ITS operon of the rRNA gene from the MALINA strains affiliated to

C. neogracilis as well as the Antarctic strains attributed by CCMP to *C. neogracilis*. Since the

5.8S is a region highly conserved at interspecific level, we identified the boundary between ITS-

1 and 5.8S based on 5.8S sequences from other *Chaetoceros* species (Moniz & Kaczmarska

2010) available in GenBank. We then constructed a phylogenetic tree based on the ITS-1 and

another phylogenetic tree consisting in a region starting at the 5' end of 5.8S and ending in the

conserved motif of helix III of ITS-2. Some sequences did not cover the entire ITS length and

were excluded from the alignment of either the ITS-1 or the 5.8S/ITS-2. The ITS-1 alignment

included 30 sequences and 227 nucleotide positions and was analysed using a Jukes Cantor

model (Jukes & Cantor 1969). For the 5.8/ITS-2 alignment the end of helix III was annotated

based on the secondary structure of the ITS-2 from *T. weissflogii* (Grunow) Fryxell & Hasle

(Sorhannus et al. 2010), which is the species most closely related to the genus *Chaetoceros* for

which the secondary structure of the ITS-2 has been reconstructed. The final alignment included

30 sequences and 384 nucleotide positions and both ML and NJ phylogenies were inferred using

a Kimura-2 model (Kimura 1980). The ITS could not be sequenced from the strain MALINA

E43.N2, but it was attributed to Clade II based on its 28S sequence. Similarly since both the ITS-

1 and the 5.8 + ITS-2 sequences from RCC2268, RCC2277 and RCC2318 were not sufficiently

long to be included in the ITS-1 and the 5.8S/ITS-2 alignments, a neighbour joining phylogenetic

tree for the entire ITS fragment which included 34 sequences for a total 483 positions (Fig. S1 in the Supporting Information) was constructed in order to identify the genetic clade of these strains.

ITS-2 structure prediction. To characterize our MALINA strains of *C. neogracilis* in deeper detail we reconstructed the secondary structure of the ITS-2 operon of the rRNA. The ITS-2 boundaries were then annotated using Hidden Markov Models of the flanking 5.8S and 28S regions (Keller et al. 2009). The secondary structure of the ITS-2 was first inferred for the strain RCC2014 using the RNA structure program (Mathews et al. 2004) and then transferred onto other *Chaetoceros* sequences through homology modelling (Wolf et al. 2005) using the ITS-2 database (Merget et al. 2012).

Microscopy. At least one strain per genotype, for a total of 61 strains (Table 1), was observed and photographed in light microscopy. Cells were harvested during the exponential phase of their growth and observed using an Olympus BX51 microscope (Olympus, Hamburg, Germany) with a 100X objective using differential interference contrast (DIC). Cells were imaged with a SPOT RT-slider digital camera (Diagnostics Instruments, Sterling Heights, MI, USA). Micrographs are available at http://www.roscoff-culture-collection.org for a large set of strains.

Selected strains, covering most genetic diversity based on both 18S and 28S rRNA, were observed using Light Microscopy (36 strains), TEM (25 strains) and/or SEM (28 strains) at Stazione Zoologica Anton Dohrn (Table 1). To remove organic matter, samples were treated

with nitric and sulfuric acids (1:1:4, sample:HNO_3:H_2SO_4), boiled for a few seconds and washed

with distilled water. LM observations were performed using a Zeiss Axiophot 200 equipped with

a Axiocam Digital Camera (Carl Zeiss, Oberkochen, Germany). Acid-cleaned material was

mounted on Formvar- coated grids and observed with a LEO 912AB transmission electron

microscope (LEO, Oberkochen, Germany) and/or mounted on stubs, sputter-coated with gold-

palladium and observed with a JEOL JSM-6500F SEM (JEOL-USA Inc., Peabody, MA, USA).

Fixed samples not subjected to cleaning were placed on Nuclepore 3 μm pore size (Nuclepore,

Pleasanton, CA, USA) polycarbonate filters, rinsed with distilled water, dehydrated in an ethanol

series (25, 50, 75, 95, and 100%), and critical-point-dried. Dried filters were mounted on stubs,

sputter-coated and observed with SEM.

RESULTS

In the present study, we characterized 75 diatom strains using a combination of morphological

and molecular techniques (Table 1). We sequenced the V4 region of the 18S rRNA from all the

strains and then we sequenced the full 18S rRNA from at least one strain from each unique

genotype. Moreover we sequenced the 28S rRNA from most of our strains and the ITS operon of

the rRNA from all the strains affiliated to *C. neogracilis.* The strains grouped into 17 genotypes

based on 18S and 28S rRNA phylogenies (Figs. 1 and 2). 28S rRNA and ITS analyses indicate

that 36 strains of *C. neogracilis* sharing identical 18S rRNA gene sequence make up 4 distinct

genetic clades (Figs. 2 and 3). The most represented genera were *Chaetoceros* and *Thalassiosira*.

Bacillariaceae. We isolated 9 Bacillariaceae strains from the genera *Cylindrotheca, Nitzschia* and *Pseudo-nitzschia.* The 18S rRNA gene (Fig. 1) discriminated the different *Cylindrotheca* and *Nitzschia* representatives but was poorly resolutive for the different *Pseudo-nitzschia* species.

Cylindrotheca closterium (Ehrenberg) Lewin & Reimann.

Cells are 85 to 108 μm long, fusiform with rostrated ends and possess two chloroplasts (Hasle 1964, Jahn & Kusber 2005). The valve face is unperforated, transversed by transapical slightly silicified ribs. The central raphe is interrupted by a central nodule. The fibulae (13-17 in 10 μm) are narrow, irregularly spaced, and joined directly to the valve face (Fig. 4A; Hasle 1964, Jahn & Kusber 2005).

Cylindrotheca closterium was considered as a cosmopolitan species but it was demonstrated to constitute a species complex of similar morphotypes belonging to different genetic lineages (Haitao et al. 2007). It has been repeatedly observed in the Arctic (Table 2).The 18S rRNA gene sequence from *C. closterium* strain RCC1985 (Fig. 1) groups with the other *C. closterium* sequences forming a moderately-supported clade (sequence similarity > 97.8 %), but does not cluster to any of the two lineages described to date for the *C. closterium* species complex (Haitao et al. 2007). The 28S rRNA gene sequence from *C. closterium* strain RCC1985 (Fig. 2A) branches with two other sequences from *C. closterium.*

Nitzschia pellucida Grunow.

Cells (apical axis: 35 μm; transapical axis: 3.0-3.5 μm) are solitary and possess two

chloroplasts. Cells are lanceolate, tapering towards the poles, in valve view (Fig. 4B), and

rectangular when observed in girdle view. The densities of fibulae and striae are 12-15 and 35-40

in 10 μm, respectively. Each stria contains one row of rounded poroids. A central larger

interspace is present (Fig. 4, C and D).

Nitzschia pellucida has been previously reported in Arctic and Antarctic waters but also in

European freshwater environments (Table 2). The 18S rRNA gene sequence from *N. pellucida*

strain RCC2276 is highly related to that of *Nitzschia dubiiformis* (99.6 % sequence identity) and

branches with other *Nitzschia* species (Fig. 1). The 28S rRNA gene sequence from *N. pellucida*

strain RCC2276 groups with *Nitzschia laevis* and *N. pellucida* from GenBank (sequence identity

97.5 and 97.4, respectively). This clade branches with different *Nitzschia* and *Cylindrotheca*

species (Fig. 2A), which supports the assertion of Lundholm et al. (2002) describing the genus

Nitzschia as polyphyletic.

Pseudo-nitzschia granii (Hasle) Hasle.

Cells (apical axis: 17-25 μm; transapical axis: 1.4-1.8 μm) have two chloroplasts and colonies

were not observed in culture conditions. Valves are lanceolate with a central swelling, one side

of the valves is linear and the other convex (Fig. 4E). Apices are rounded. The striae (54-55 in 10

μm) are composed of a single row of poroids divided in 5-7 sectors. In the strain RCC2006, most

of the valves have striae barely silicified that lack complete poroids (Fig. 4F) or have few

poroids entirely formed (Fig. 4G). The fibulae (16-18 in 10 µm) are irregularly spaced and the central interspace is absent.

Pseudo-nitzschia granii has been reported in northern cold waters, including Arctic and subarctic regions (Table 2).

Pseudo-nitzschia arctica Percopo & Sarno.

Four *Pseudo-nitzschia* strains isolated during the MALINA cruise have been recently described as a new species, *Pseudo-nitzschia arctica* (Percopo et al. 2016). Cells occur in colonies and each cell overlaps the next sibling cell for ca 1⁄8 of its length (Fig. 4H). Cells (apical axis: 26-60 µm; transapical axis: 1.6-2.5 µm) are lanceolate in valve view. The valve ends are broadly pointed. The fibulae are not always regularly spaced. The two central fibulae have a larger interspace and the raphe is here interrupted by a central nodule (Fig. 4I). The densities of fibulae and interstriae are 17-24 and 34-39 in 10 µm, respectively. The striae contain 1 row of rounded poroids, 5-6 poroids in 1 µm. Each poroid most often contains 1-6 sectors. Some striae are simply composed of more lightly silicified areas without any perforations.

Pseudo-nitzschia arctica seems to have a distribution confined to the northern polar area, possibly representing one of the endemic components of the Arctic diatom flora (Percopo et al. 2016).

Pseudo-nitzschia arctica and *P. granii* share highly similar 18S rRNA gene sequences (99.6 % sequence identity, Fig. 1) and the two species can be better separated using 28S rRNA phylogeny (Fig. 2A) where their sequences differ by 1.2 % sequence identity.

Fragilariaceae.

Synedropsis hyperborea (Grunow) Hasle, Medlin & Syvertsen.

Cells (apical axis: about 55 µm; transapical axis: 2.7-3.5 µm) are lanceolate in valve view (Fig. 4J). No colonies were observed. The uniseriate striae (22-23 in 10 µm) are parallel towards the apices and alternate in the some parts of the valve (Fig. 4K). The apical fields are composed of 5-7 slits (Fig. 4, L-N) slightly different from that reported in the original description (4-6 slits, Hasle et al. 1994). A single rimoportula is located two or three striae from one of the two valve apices (Fig. 4L). The rimoportula opens externally into a hole larger than the surrounding areolae (Fig. 4, M and N).

Synedropsis hyperborea is typical of the Northern cold region and it is commonly reported in Arctic waters (Table 2).

Fragilariaceae taxonomy was not well resolved based on 18S rRNA gene since the sequence from *S. hyperborea* strain RCC2043 shares very high similarities with a sequence from Genbank affiliated to *S. hyperborea* (99.9 %) as well as *Synedra minuscula* (99.9 %), *Fragilaria* sp. (99.9 %) and *Grammonema striatula* (99.5 %, Fig. 1). MALINA strains RCC2043 and RCC2520 belonging to *S. hyperborea* share identical 28S rRNA gene sequences and group with a sequence from *Synedropsis hyperboreoides* from GenBank (98.5 % sequence identity). The 28S rRNA gene sequences from these strains are also related to *Thalassionema frauenfeldii* and 3 *Fragilaria* species (Fig. 2A).

Attheyaceae.   *Attheya septentrionalis* (Østrup) Crawford.

Cells (apical axis: 3.5-6.4 μm; pervalvar axis: 7-11.7) are solitary and bear four slightly wavy horn-like projections (Fig. 5, A and B). One or two plate-like chloroplasts are present. Valves are almost circular and lack the rimoportula (Fig. 5C). The length of the horns is variable (12-35 μm) and the ratio between horn length and cell diameter ranges from 2.9 to 4.4. The number of longitudinal strips can be 3 or 4 in both examined strains (Fig. 5, D and E).

Attheya septentrionalis is distributed in the northern cold region and it is common in Arctic waters (Table 2).The 18S rRNA gene from the MALINA strains RCC1986 and RCC2042 branches with that of sequences of *A. septentrionalis* (99.9 % sequence identity) and *Attheya longicornis* (99.8 %) from GenBank and is related to sequences from three *Biddulphia* spp. (Fig. 1). The 28S rRNA gene from the two MALINA strains is also highly related to that of sequences of *A. septentrionalis* and *A. longicornis* (≈ 98 % sequence identity, Fig. 2A).

Thalassiosiraceae. We isolated 12 Thalassiosiraceae strains (Table 1) affiliated to the genera *Thalassiosira, Porosira,* and *Shionodiscus*. Both 18S and 28S rRNA gene allowed the discrimination of the different species found here (Figs. 1 and 2B).

Thalassiosira gravida Cleve.

Cylindrical cells (diameter: 28.5-30.5 μm) held in colonies by a single thick thread composed of several strands (Fig. 5F). A number of fultoportulae (or strutted processes, 11-15) are grouped in a central cluster and several fultoportulae are scattered on the valve face. The marginal fultoportulae are arranged to form 3-4 rings placed between the margin of the valve face and the mantle. A single rimoportula (or labiate process) is located within the inner ring of marginal

fultoportulae (Fig. 5G). Different valves have a variable degree of silicification, but in general the areolae are well-formed on the margins of the valve (16-20 in 10 µm) and poorly developed in the central part, where siliceous radial ribs separate perforated areas.

Thalassiosira gravida is regarded as a bipolar, cold to temperate water species and it has been previously observed in Arctic and Antarctic waters (Table 2).

The 18S rRNA gene sequence from *T. gravida* strain RCC1984 clusters with sequences from both *T. gravida* and *T. rotula* (sequence identity > 99.5 %) and is highly related with a sequence from *Thalassiosira eccentrica* (99.3 % sequence identity, Fig. 1). The 28S rRNA gene sequences from both our strains of *T. gravida* group with two other sequences from *T. gravida* and are highly related to 2 sequences from *T. rotula* (99.2 % sequence identity, Fig. 2B).

Thalassiosira cf. *hispida* Syvertsen.

Cells (diameter: 6.5-13.5 µm) possess several chloroplasts, and form colonies of few cells (3-4 cells) connected by one central thread. The areolae (30 in 10 µm) have a similar size on both valve face and mantle. One ring of marginal fultoportulae (5 in 10 µm) and one central fultoportula are present on the valve face (Fig. 5H). The marginal fultoportulae have long external tubes (Fig. 5, H-K). All the fultoportulae have four satellite pores at their base (Fig. 5I). The rimoportula is positioned slightly inside the ring of marginal fultoportulae, between two of them. It can be either closer to one of them or in the middle. A broad hyaline margin is present. Short and minute spines and hairs emerge throughout the valve (Fig. 5I). The girdle is formed by a valvocopula, a copula and several open bands. The valvocopula has a broad abvalvar imperforated rim and one advalvar row of areolae (Fig. 5J). MALINA strain of *T.* cf. *hispida* is

morphologically very similar to the original description of *T. hispida* but possesses a higher

number of areolae (18 and 24-26 in 10 μm on valve face and mantle, respectively, in Syvertsen

1986). Very similar is the dense covering of spinules on the valve surface, which however is not

specific for *T. hispida*, but can be developed to a lesser extent in other *Thalassiosira* species, and

the presence of a broad hyaline margin on the valve and a valvocopula with a wide non-pierced

edge.

Thalassiosira hispida has only been reported in northern cold water regions (Table 2). 18S

rRNA gene sequences from *T. hispida* are not available on the GenBank and the 18S rRNA gene

sequence from our strain RCC2521 clusters with sequences of *Thalassiosira allenii* (98.5 %

sequence identity) and *Thalassiosira angulata* (98.6 %, Fig. 1). The 28S rRNA gene sequence

from RCC2521 (Fig. 2B) groups with *T. allenii* (97.5 %), *Thalassiosira aestivalis* (97.1 %) and

T. nordenskioeldii (96.5 %) but the clade is poorly (< 50 % ML and NJ) supported.

Thalassiosira minima Gaarder.

Cells (diameter: 4.5-13μm) have two chloroplasts and do not form colonies under our culture

conditions. In girdle view, cells are rectangular with a pervalvar axis generally shorter than the

cell diameter and with a valve face slightly depressed in the centre (Fig. 5L). The areolae (30-35

in 10 μm) are hexagonal in shape (Fig. 5M). On the valve, a ring of marginal fultoportulae (4-6

in 10 μm) with short external tubes and one or two central fultoportulae are present (Fig. 5, M

and N). Five fultoportulae have been occasionally observed in one single valve (Fig. 5O). A

large rimoportula is placed between two marginal fultoportulae, slightly closer to one of them

(Fig. 5, M and N). Each marginal fultoportula is accompanied with a small external labiate-

shaped protrusion (Fig. 5P). The species has a worldwide distribution (Table 2) and it is reported for the first time in the Arctic Ocean.

The 18S rRNA gene sequence from our *T. minima* strain RCC2265 is highly similar to that of the *T. minima* sequence from the strain CCMP990 (99.7 %, Fig. 1). Our strains of *T. minima* from both the Beaufort Sea and the North Pacific Ocean (Table 1) share highly similar 28S rRNA gene sequences with the Antarctic strain RCC2707 (99.1 %) and group with the *T. minima* strain CCMP990 forming a well-supported clade (Fig. 2B). Consistent with the 18S rRNA gene phylogeny, *Thalassiosira curviseriata* is the species most closely related to all the *T. minima* strains.

Thalassiosira nordenskioeldii Cleve.

Cells (diameter: 12-15 µm) possess several chloroplasts and form long colonies connected by a central thread (Fig. 6A). Areolae are 17-18 on valve face and 18-20 in 10 µm on mantle (Fig. 6B). Valves are characterized by a pronounced concavity in the centre, a high (4-6 areolae) and oblique mantle, a marginal ring of fultoportulae (3-4 in 10 µm) with long external tubes bearing a terminal collar, one central fultoportula and one rimoportula positioned within two marginal fultoportulae (Fig. 6, B and C).

Thalassiosira nordenskioeldii is a species typical of northern cold to temperate regions, common in Arctic waters (Table 2).

The 18S rRNA gene sequence from strain RCC2000 groups with sequences from *T. aestivalis* and *T. nordenskioeldii* forming a well-supported clade (Fig. 1). *Thalassiosira nordenskioeldii* RCC2000 shares identical 28S rRNA gene sequence with another *T. nordenskioeldii* strain from

the GenBank and highly similar 28S sequence (99.8 %) with *T. nordenskioeldii* RCC2021. These

strains form a clade with a sequence from *T. aestivalis* (Fig. 2B).

Porosira glacialis (Grunow) Jørgensen.

Cells (diameter: 30-40 μm) are cylindrical, possess several chloroplasts and can form short

colonies (2-3 cells; Fig. 6, D and E). Numerous fultoportulae are scattered over the valve surface

(3-4 in 10 μm). The striae (24-27 areolae in 10 μm) are wavy and radially arranged. A central

annulus is present and a large rimoportula process is situated inside the margin of the valve (Fig.

6F).

Porosira glacialis is reported in Arctic and Antarctic waters (Table 2).

RCC2039 18S rRNA is identical with that from the Antarctic strain CCMP1099 (Fig. 1). The

28S rRNA gene sequence from the MALINA strain RCC2039 is highly related, but not identical

(99.6 %), to that of the two Antarctic strains CCMP1099 and RCC2709 (Fig. 2B).

Shionodiscus bioculatus (Grunow) Alverson, Kang & Theriot.

Cells (diameter: 23-41 μm) are solitary and possess a large number of discoid chloroplasts

(Fig. 6G). The pervalvar axis is generally longer than the diameter. The valve face is slightly

convex and the mantle is rounded. The areolation is fasciculate (20-23 areolae in 10 μm) with a

single fultoportula in the valve centre and a subcentral rimoportula (Figs. 6, H and I). The

marginal fultoportulae (4-7 μm apart) have internal tube-like projections and no external

extensions. Strain RCC1991 is the first representative of *S. bioculatus* sequenced to date, both

18S and 28S rRNA gene sequences from this strain group with sequences of *Shionodiscus*

oestrupii and *Shionodiscus ritscheri* (Figs. 1 and 2B).

Cymatosiraceae.

Arcocellulus cornucervis. Hasle, von Stosch &Syvertsen.

Cells are solitary, very small (apical axis: 3.0–3.5 µm; pervalvar axis: 1.4-1.7 µm; transapical axis: 1.7-2.2 µm) and slightly curved in broad girdle view. Each cell possesses two different valves, a process valve and a pili valve, which are convex and concave, respectively, in larger cells (Fig. 6, J and K). Each valve has two ocelluli (Fig. 6, K and L). The pili cross each other and bear conspicuous branches (Fig. 6J). The process valve possesses a central process (Figs. 6K and 7A). A marginal row of poroids is always present along the margin of the valve and a variable number of poroids can be present on the valve face. The basal siliceous layer may be smooth or ornamented by costae which can be indistinct or more convoluted (Fig. 6K). Costae seem to be more pronounced in process valves. Patches of short spinules can be present near the pilus base (Fig. 7A).

Arcocellulus cornucervis has been reported in temperate and cold waters of both hemispheres, including Arctic Ocean (Table 2).

18S phylogeny could not discriminate *Arcocellulus* spp. from the closely related genus *Minutocellulus* (Fig. 1). The 18S rRNA gene sequence from *A. cornucervis* RCC2270 is indeed highly related to two sequences from *Minutocellus polymorphus* (99.5 % sequence identity) and both form a well-supported (96% ML, 100 % NJ) clade which branches with that of other representatives from the family Cymatosiraceae, namely *Papiliocellulus elegans*, *Cymatosira belgica*, and *Brockmanniella brockmanni* (Fig. 1).

The 28S rRNA gene of *A. cornucervis* strain RCC2270 is closely related to that of two unidentified Cymatosiraceae (95 and 95.9 % sequence identity) isolated from temperate waters (Fig. 2B).

Hemiaulaceae.

Eucampia groenlandica Cleve.

Cells (apical axis: 7-24 µm) are rectangular in girdle view, slightly silicified and possess several chloroplasts. Cells form colonies which can be straight or slightly curved in broad girdle view with square to hexagonal apertures (Fig. 7B). A rimoportula is present on the centre of the valve (Fig. 7C).

Eucampia groenlandica was first reported from Baffin Bay in Davis Strait and is considered typical of the northern cold waters (Table 2).

The 18S rRNA gene sequence from *E. groenlandica* strain RCC1996 groups with sequences of *Eucampia zodiacus* (99.2 %) and *Eucampia antarctica* (99.0 %) forming a well-supported clade (Fig. 1). The 28S rRNA gene from our strains is related to a sequence from *E. zodiacus* (96.9 % sequence identity, Fig. 2B).

Chaetocerotaceae. We isolated 45 strains of the genus *Chaetoceros* and using the 28S rRNA (Fig. 2B, and 3A) and ITS phylogeny (Fig. 3, B and C) we grouped these strains into 6 genotypes, 2 of them corresponding to the species *Chaetoceros decipiens* and *C. gelidus* respectively, and 4 other being closely related genotypes affiliated to *C. neogracilis*.

Chaetoceros decipiens Cleve.

Cells (apical axis: 11-22 µm) were generally solitary in culture conditions but a few colonies have been observed (Fig. 7, D and E). Each cell possesses several chloroplasts. Chains are straight and the apertures are elliptical. All setae lie in the apical plane. The intercalary setae emerge from the valve margin without a basal part and may fuse for a shorter or longer distance. Terminal setae are U or V shaped (Fig. 7, D and E). The valve, with a high mantle, is almost flat in girdle view (Fig. 7, F and G). Valves have a central annulus from which irregular ribs radiate and are perforated with small poroids. The mantle is high and a marginal ridge is present between the valve face and mantle (Fig. 7F). Terminal valves possess a very small central process with a short external projection (Fig. 7H). Girdle bands are ornamented with parallel transverse costae interspaced by hyaline areas with scattered small poroids (Fig. 7I). The setae are polygonal, mostly four-sided, in cross section, with spines on the edges and a single longitudinal row of large pores on each side.

Chaetoceros decipiens is a cosmopolitan species, common in arctic waters (Table 2).

The 18S rRNA gene sequence from our strain of *C. decipiens* (RCC1997) groups with a GenBank sequence from *Chaetoceros* cf. *lorenzianus* (97.1 % sequence similarity, Fig. 1) and, similarly, the 28S rRNA gene is closely related to GenBank sequences from *Chaetoceros lorenzianus* (99.2 %), and groups with *Chaetoceros affinis* and *Chaetoceros diadema* (Fig. 2B).

Chaetoceros gelidus Chamnansinp, Li, Lundholm & Moestrup.

Cells (apical axis. 4-12 µm) with a single lobed chloroplast are joined in curved chains (Fig. 7J). Several chains group together forming a spherical colony (Fig. 7 K). The setae emerge inside the valve margin and merge after a short basal part forming narrow hexagonal apertures (Fig. 7L). In valve view, the valve is circular to oval, in girdle view it is slightly concave with a small

central inflexion (Figs. 7L and 8A). Generally the cells have three short curved setae and one long straight seta. The short setae have densely spirally arranged spines occurring throughout its length. In contrast the long straight seta does not exhibit spines on its basal part, whereas on its distal part it possesses spines which are more distant between each other (Fig. 8B). Both valves from each resting spore are convex and smooth.(Fig. 8C). The crest reported in the original description (Chamnansinp et al. 2013) is absent here. Variability in spore morphology of *C. gelidus* was already reported (Degerlund et al. 2012, therein as *C. socialis*, northern strains).

The species has been reported from northern cold waters, including Arctic Ocean (Table 2).

The 18S sequence of *C. gelidus* clusters with a sequence of *C. socialis* (97.2 % sequence identity, Fig. 1) and 28S rRNA sequences are identical to that of the type strain of *C. gelidus* (Fig. 2B).

Chaetoceros neogracilis (Schütt) VanLandingham.

Twenty-eight of the 36 strains of *C. neogracilis* isolated here have been observed by LM and photographs are available for most of them (http://www.roscoff-culture-collection.org). Seven strains have been further examined using EM (Table 1). Cells are generally solitary (Fig. 8, D-F) but short colonies (3-6 cells) have been occasionally observed (Fig. 8G) in 9 strains. Cells are relatively small (apical axis: 4-12 µm) and possess a single lobed chloroplast (Fig. 8, D-G). No significant morphological and ultrastructural difference has been observed among the different strains, with the exception of a certain variability in the orientation of the setae. As single cells, some strains have straight setae diverging at an angle of 45°, whereas others have setae perpendicular to pervalvar axis, and others have more curved setae (Fig. 8, D-F), but this variability might be associated to the different cell sizes of the strains. In the colonies, cells are joined to form straight chains and they are separated by apertures varying from elliptically

shaped (Fig. 8, G and H) to narrow slits (not shown). Terminal setae are U or V shaped. Valves are ornamented with irregular costae originating from a central annulus. In the terminal valves, a slit-like process is located in the centre of the annulus and it bears an external flattened tube (Fig. 8, I and J). The central process is absent in the intercalary valves of the colonies, confirming that the chains are real colonies and not cells in division (Fig. 8K). Intercalary setae originate from the valve apices, cross immediately at the chain margin and diverge running in different directions (Fig. 8, H and L). The setae are circular in cross section. They are composed by long spiral costae ornamented with arrowhead-shaped spines (about 2 spines per 1 μm) and interconnected by short transverse costae (Fig. 8, M and N). Spores were not observed in any of the tested strains.

The name *C. neogracilis* (basionym: *C. gracile* Schütt) has been attributed almost indiscriminately to many small, unicellular *Chaetoceros* taxa collected worldwide (see Rines & Hargraves 1988 for a discussion). The specific epithet can be found in the literature spelled as *C. gracile* or *C. neogracile*, because the genus *Chaetoceros* was considered to be neutral, rather than masculine. However the genus is currently recognised as a masculine word and the correct name of the species is *C. neogracilis*. In more recent years, the species has been consistently reported as a significant component of microbial communities in Arctic and Baltic (Table 2) as well as Antarctic regions.

All the *C. neogracilis* strains isolated during the MALINA cruise share 100% identity in the V4 region of the 18S rRNA gene (data not shown). The full 18S rRNA gene has been sequenced for strains RCC2016 and RCC2318. These two MALINA strains share identical 18S rRNA gene sequence with the two Arctic strains ArM0004 e ArM0005 and form a well-supported clade with the sequence from the Antarctic strain AnM0002 (98.9 % sequence identity, Fig. 1). The

28S rRNA gene sequences from the MALINA strains of *C. neogracilis* cluster together (Fig. 2B) as well as with a GenBank sequence from the Baltic strain CPH9 attributed to *C. fallax* (Chamnansinp et al. 2013) and have a sister clade which includes the sequences from three Antarctic strains (CCMP163, CCMP189 and CCMP190). All these sequences branch with *Chaetoceros tenuissimus* forming a well-supported clade (Fig. 3A).

Genetic diversity of Chaetoceros neogracilis *strains.* The MALINA strains of *C. neogracilis* shared highly similar although not identical 28S rRNA gene sequence. Sequences can diverge by up to 0.5 %. Both ITS markers as well as 28S rRNA gene indicate significant differences between the Arctic and the Antarctic strains (Fig. 3), since the two groups form two separate branches. For example the Arctic *C. neogracilis* RCC2014 shares with the Antarctic strain *Chaetoceros* sp. CCMP189 95 %, 86 %, and 85 % sequence similarity for the 28S, ITS-1, and 5.8S + ITS-2, respectively. The MALINA strains of *C. neogracilis* form four different clades based on all the three markers used. Overall, based on either or both 28S rRNA (Fig. 3A) and ITS phylogeny (Figs. 3, B and C, S1), 20 strains belong to Clade I, 8 to Clade II, 2 to Clade III and 6 to Clade IV (Table 1). The 28S rRNA gene phylogeny (Fig. 3A) separates the *C. neogracilis* strains in two groups, both with high (> 75 % in both ML and NJ) bootstrap support. One group consists of *C. neogracilis* Clade I, whereas the second group includes the other 3 clades. Specifically strains from Clade II are at the base of the group from which Clade III and Clade IV emerge with moderate (> 50 %) support in both ML and NJ (Fig. 3A). The strain CPH9 falls within Clade II and the Antarctic strains CCMP163, CCMP189 and CCMP190 are fully separated from *C. neogracilis*. Both ITS-1 and 5.8S + ITS-2 trees includes 27 Arctic sequences from *C. neogracilis*, with 15 of them forming Clade I, 4 strains belonging to Clade II, 2 strains to Clade III, and 6 strains to Clade IV. Strains from each clade cluster between them with moderate

support in ITS-1 phylogeny and Clade II, Clade III, and Clade IV group together with high

bootstrap support (Fig. 3B). In 5.8S+ITS-2 phylogeny Clade II and Clade III are highly

supported, whereas Clade I and Clade IV are moderately supported; Clade III groups with Clade

I and some differences occur between the different strains from Clade II (Fig. 3C).

Secondary structure of ITS-2. We predicted the secondary structure of ITS-2 rRNA for our

strains of *C. neogracilis* to further investigate their genetic differences. We determined

Compensatory Base Changes (CBC) and Hemi-CBC in positions paired in the helices of the

secondary structure according to Coleman (2009). The secondary structure of ITS-2 from our

strains exhibits four helices (I, IIa, III and IV) typical of all eukaryotes (Coleman 2009) as well

as an additional helix (IIb) located between helix IIa and helix III (Fig. 9). Differences in the

ITS-2 sequences from our strains occur at 14 positions, 9 of them located in paired positions of

the helices. This variability in paired positions consists in Hemi-CBC for 6 nucleotides, and CBC

for 2 nucleotides. Two hemi-CBC occur in helix I (GC ↔ AC, and CG ↔ UG), 3 in helix III

(CG ↔ UG, GC ↔ GU, GU ↔ AU), and 1 in helix IV (GU ↔ GC). Moreover 1 CBC occurs on

helix IIa between clade I and II (AU) versus clade IV (GC), with clade III showing a Hemi-CBC

(GU) towards the other three clades (Fig. 9).

DISCUSSION

Combining microscopy and genetic data. The combination of morphological and molecular

approaches on phytoplankton strains isolated during the MALINA cruise allowed the

characterization of cultured diatoms from the Beaufort Sea. To date about 10^4 species have been

described based solely on their morphology (Guiry 2012) and the application of molecular

approaches during the last decade revealed a considerable genetic diversity within key planktonic

morphospecies such as *Asterionellopsis glacialis* (Castracane) Round (Kaczmarska et al. 2014), *Leptocylindrus danicus* Cleve (Nanjappa et al. 2013)*, Pseudo-nitzschia pseudodelicatissima* (Lundholm et al. 2003, Lundholm et al. 2006, Amato & Montresor 2008, Lundholm et al. 2012, Lim et al. 2013, Orive et al. 2013), and *Skeletonema costatum* (Sarno et al. 2005, Sarno et al. 2007, Kooistra et al. 2008). It has been suggested that the number of extant diatom species exceeds by one order of magnitude those described to date (Mann & Vanormelingen 2013).

Our work provides both 18S and 28S rRNA gene sequences validated with detailed morphological and ultrastructural information for 17 morphotypes. Both genes have been sequenced here for the first time for 6 diatom species (*A. cornucervis, C. decipiens, E. groenlandica, S. bioculatus,* and *T.* cf. *hispida*). The 18S gene of *C. gelidus*, *N. pellucida*, and *P. arctica* has been also sequenced for the first time. Moreover, most of the gene sequences obtained from the Arctic strains were different from sequences from conspecific strains collected from different geographic areas that are available in GenBank. Finally, we investigated the genetic rRNA diversity of 36 *Chaetoceros* strains sharing the same 18S gene sequence, and clarified the identity of *C. neogracilis*, a taxon that dominated genetic libraries from the Beaufort Sea.

Genetic markers and species delimitation. The taxonomic resolution of the genetic markers used here was different according to the genus investigated, but it also varied within a given genus, depending on the phylogenetic distance existing between congeneric species.

The 18S rRNA gene can successfully discriminate species within the genus *Nitzschia* (Rimet et al. 2011) and the *C. closterium* species complex (Haitao et al. 2007). Both 18S and 28S rRNA genes are commonly used for the taxonomic identification of *Thalassiosira* species (Kaczmarska et al. 2006, Alverson et al. 2007, Hoppenrath et al. 2007) and here they provided a good

taxonomic resolution for all the Thalassiosiraceae representatives except *T. gravida*, which shares identical 18S rRNA gene with *T. rotula* (Fig. 1). These two species show low phylogenetic distances also on 28S rRNA gene phylogeny (Fig. 2B) and can be correctly separated only after ITS sequencing (Whittaker et al. 2012).

The 28S rRNA gene is a relatively good molecular marker to discriminate most of *Pseudo-nitzschia* species although a better resolution of phylogenetic relationships can be generally achieved with the ITS rRNA possibly supplemented by the analysis of the secondary structure of the ITS2 (Lundholm et al. 2003, Amato et al. 2007, Lundholm et al. 2012, Lim et al. 2013, Orive et al. 2013, Percopo et al. 2016). *Pseudo-nitzschia arctica* and *P. granii* share highly similar 18S rRNA gene sequences (Fig. 1) but can be better discriminated based on 28S rRNA (Fig. 2A), ITS and *rbc*L phylogenies (Percopo et al. 2016).

Similarly, the MALINA strains of *C. neogracilis* and two Arctic strains isolated from the Greenland Sea (EU090013 and EU090014; Choi et al. 2008) share identical 18S rRNA sequences (Fig. 1), but they are genetically different at both 28S and ITS levels (Figs. 2B, and 3). 28S and ITS rRNA phylogenies consistently grouped sequences from the Arctic strains of *C. neogracilis* into four phylogenetically discrete clades (Fig. 3). The differences in the ITS secondary structure confirm this grouping and would indicate reproductive isolation between the four clades of *C. neogracilis* which may correspond to closely related but distinct cryptic species. Specifically a CBC in helix IIa (Fig. 9) suggests reproductive isolation between clade I and clade II vs. clade IV, and similarly the presence of at least a Hemi-CBC in the Helix III between Clade I and Clade II, as well as between Clade III and all the other clades, suggests that the different clades are unable to interbreed (Coleman 2009). The secondary structures of both ITS-1 and ITS-2 are involved in ribosome assembly (Tschochner & Hurt 2003) and changes in paired positions

likely affects gamete compatibility preventing cells differing by CBC or Hemi-CBC from mating (Coleman 2001). For diatoms, inability to interbreed has been demonstrated between strains differing by CBC or Hemi-CBC in the ITS-2 within the *P. pseudodelicatissima* species complex (Amato et al. 2007).

The sympatric occurrence of distinct genetic clades of *C. neogracilis* in the Beaufort Sea gives further support to the hypothesis that they should be considered separate species unable to interbreed rather than different genotypes of a single species. Closely-related species or genotypes can co-occur in the same environment and similar results were found previously in dinoflagellates. Several ITS genotypes from the Atama complex, which consisted of *Alexandrium tamarense* (Lebour) Balech, *Alexandrium fundyense* Balech*,* and *Alexandrium catenella* (Whedon & Kofoid) Balech*,* co-occurred in the Chukchi Sea (Gu et al. 2013). In contrast, the Arctic *Micromonas* (Lovejoy et al. 2007, Balzano et al. 2012b) consisted in a single ITS genotype (Balzano et al. 2012a), which dominated both surface and DCM, waters throughout the Beaufort Sea during the MALINA cruise (Balzano et al. 2012b).

Notably, clone libraries based on 18S rRNA gene sequences, and high throughput amplicon sequencing of the V4 or V9 regions of the 18S rRNA, which are widely used in environmental studies (Stoeck et al. 2010, Comeau et al. 2011, Logares et al. 2012, Logares et al. 2014, Balzano et al. 2015), failed to discriminate among the four clades of *C. neogracilis* and recovered them as a unique genotype (Pawlowski et al. 2008, Lovejoy & Potvin 2011).

Both 18S and 28S rRNA genes are too conserved for some genera failing to discriminate the different species. For example, *A. septentrionalis* shared identical 18S rRNA and 28S rRNA gene sequences with *A. longicornis* (Figs 1, and 2A). These two species can be distinguished

only using a combination of several nuclear and plastidial encoded genes (Sorhannus & Fox 2012).

The 18S rRNA gene is highly conserved also within the family Cymatosiraceae, where *A. cornucervis* strain RCC2270 shares almost identical 18S rRNA with two GenBank sequences from *M. polymorphus* (Fig. 1), and the 2 species share 100% identity in the V4 region (Luddington et al. 2012). The extent of the variability of the 28S rRNA gene within the Cymatosiraceae is not clear since no other sequence from this family is available on GenBank and *A. cornucervis* RCC2270 shares highly similar 28S rRNA gene with two unidentified Cymatosiraceae strains (Fig. 2B).

Overall, ITS-2 provides a higher taxonomic resolution than 28S, but although it was proposed as a universal barcode for diatoms (Moniz & Kaczmarska 2010, Guo et al. 2015), very few ITS sequences are available to date in GenBank compared to 18S and 28S and its high variability makes the alignment between different genera difficult or even impossible. Similarly the 28S rRNA gene is less conserved than the 18S rRNA allowing a better discrimination between congeneric species but 28S sequences are available for a larger number of diatom species. Ideally sequencing the entire rRNA operon from the same specimen would allow the best taxonomic resolution and provide taxonomic annotation from most species in environmental studies. Single molecule sequencing technologies such as PacBio could allow the sequencing of reads as long as 5,000 bp (Mikheyev & Tin 2014, Schloss et al. 2016). For current sequencing technologies the 28S rRNA seems the best compromise between resolutive power and easiness of alignment, for environmental studies focused on diatoms, whereas 18S rRNA gene sequencing can be used for general studies on microbial eukaryotes.

Diatoms in the Beaufort Sea. Diatoms represented an important fraction of the nano- and microphytoplankton identified during the MALINA cruise (Balzano et al. 2012b, Coupel et al. 2015) with *Chaetoceros* and *Thalassiosira* being the most represented genera. Different species from these two genera are frequently observed in Arctic waters where they typically dominate phytoplankton assemblages (Booth & Horner 1997, Lovejoy et al. 2002, Ratkova & Wassmann 2002), eventually forming spring blooms (Booth et al. 2002, Sukhanova et al. 2009).

In spite of the high diversity reported in previous studies (Sukhanova et al. 2009), only few environmental ribotypes associated with *T. nordenskioeldii* were detected by T-RFLP among sorted photosynthetic eukaryotes during the MALINA cruise (Balzano et al. 2012b) and only *T. nordenskioeldii, T. gravida*, *Thalassiosira pacifica* and few undetermined species were observed by microscopy counts (http://malina.obs-vlfr.fr), accounting for a low proportion of the phytoplankton community. Clearly, *Thalassiosira* species did not bloom in the Beaufort Sea during late summer 2009 and *T. gravida, T.* cf. *hispida,* and *T. minima* were possibly only present in low abundance.

The high number of *Chaetoceros* strains (45), mostly represented by *C. gelidus* and *C. neogracilis*, reflected the dominance of these two species in the summer phytoplankton assemblages, already shown by the genetic libraries (Balzano et al. 2012b). Notably, phytoplankton counts confirmed the high abundance of *C. gelidus* and other unidentified morphotypes, but barely reported the occurrence of *C. neogracilis*. This discrepancy indicates that cells of *C. neogracilis* might have been erroneously attributed to several different solitary species, such as *C. tenuissimus* or *Chaetoceros simplex* Ostenfeld, or other undetermined *Chaetoceros.* We also suggest that cell chains of *C. neogracilis*, which were described for the first time in this study, might have been wrongly identified as the freshwater species

Chaetoceros wighamii Brightwell (http://malina.obs-vlfr.fr; see Bosak et al. 2015 for a discussion on *C. wighamii*). Similarly, the doubtful reports of *C. wighamii* from the Baltic Sea and Danish waters could indeed refer to *C. neogracilis*, as suggested by the morphological and ultrastructural similarity between Arctic strains of *C. neogracilis* described in this study and culture material from Danish waters attributed to *C. wighamii* (see fig. 224 in Jensen & Moestrup 1998).

Other colonial *Chaetoceros* species found in the phytoplankton counts were not isolated in this study because they might be more difficult to bring into culture compared to *C. gelidus* and *C. neogracilis,* or because they are rare, as suggested by their absence in the 18S rRNA libraries and in T-RFLP analyses (Balzano et al. 2012b).

Interestingly most of the *C. neogracilis* strains from Clade I and Clade II as well as all the strains of Clade IV were isolated from surface waters (Table 1), whereas 5 out of 8 strains of *C. gelidus* and both *C. neogracilis* Clade III strains were isolated from DCM waters. During the MALINA cruise surface waters were warmer, less saline (Table S1), and poorer in nutrients (http://malina.obs-vlfr.fr/data.html) compared to DCM waters. We do not know whether these patterns are indicative of ecological preferences for these genotypes. However surface genotypes might be adapted to lower salinities, higher irradiation, higher temperatures and lower nutrient concentrations. Unfortunately, the different clades of *C. neogracilis* have identical T-RFLP ribotypes and therefore their relative contribution to the environmental samples from the MALINA cruise (Balzano et al. 2012b) cannot be discerned.

Notably, some of the strains isolated here show similarities with specimens from other environments affected by seasonal salinity shifts similar to those characterizing the Beaufort Sea. One of the *C. neogracilis* strains belonging to Clade II, CPH9 (Fig. 3A), was isolated in the

Baltic Sea, and *C. closterium* RCC1985 forms a clade, in the 28S rRNA tree, with a strain (K-520, Fig. 2A) which has been isolated from Kattegat (Lundholm et al. 2002). Interestingly, a number of environmental sequences as well as photosynthetic flagellates isolated from the surface waters of the Beaufort Sea during the MALINA cruise are genetically related to strains or environmental sequences from the Baltic Sea (Balzano et al. 2012a, Balzano et al. 2012b). Despite the significant differences in temperature and salinity between the Beaufort Sea and both the Baltic Sea and the Kattegat, the genetic similarities found in samples from these areas might be associated with the seasonal ice and the shifts in salinity occurring in these environments.

The Chaetoceros neogracilis species complex. *Chaetoceros neogracilis* was originally described as *Chaetoceros gracile* Schütt from the Baltic Sea as solitary, small *Chaetoceros* species (Schütt 1895). Due to the scanty original description and to the lack of distinctive features in such small single cell-taxa, the name has most probably been attributed to different and not related taxa collected worldwide (Rines & Hargraves 1988). All the Arctic strains isolated during the MALINA cruise share a similar cell morphology with *C. neogracilis*, together with a prevalent absence of colony formation. Indeed, *C. neogracilis* was originally described as a solitary species whereas some of the MALINA strains have been observed forming short colonies. Notably, the ability to occasionally form colonies is common to other *Chaetoceros* species considered solitary, as it has also been observed in the related species *C. tenuissimus* (D. Sarno, pers. observation). The original description of the species (Schütt 1895) includes a spiny spore that unfortunately has not been observed in our study.

Based on the available information, it is not possible to provide the authoritative taxonomic revision required by the International Code of Nomenclature for algae, fungi, and plants (McNeill et al. 2012) to establish each of the four clades as valid species and to assess if one of

them corresponds to *C. neogracilis* sensu stricto. Further analyses are required to provide additional ultrastructural information on a larger number of strains from the four clades to be compared with the type material of *C. neogracilis* and eventually designate an epitype. In the meantime, we propose that the Arctic *Chaetoceros* strains sharing very similar morphology and molecular signatures described here are considered as affiliated to *C. neogracilis* species complex. The provisional ascription of the name *C. neogracilis* to the Arctic *Chaetoceros* complex is supported by the fact that one of the strains (i.e., CPH9, syn K-1665, http://www.sccap.dk/) belonging to Clade II of the species complex, was isolated from Danish waters in the Baltic Sea, which is the type locality of *C. neogracilis*. The morphologically similar Antarctic species, which has been frequently identified as *C. neogracilis* and is represented in this study by the strains AnM0002, CCMP187, CCMP189 and CCMP190 (Choi et al. 2008), corresponds to a related but genetically distinct (Figs. 1, 2B, and 7) and probably undescribed species, here named as *Chaetoceros* sp.

Biogeography of Arctic diatoms. Most of the diatom species (10 out of 17) characterized in this study have a distribution confined to the northern/polar area, including *Pseudo-nitzschia arctica* (Percopo et al. 2016), and the *C. neogracilis* species complex, which was one of the few Arctic phylotypes identified by their 18S rRNA gene (Lovejoy & Potvin 2011) (Table 2). In addition, the MALINA strain of *C. closterium* (RCC1985) is phylogenetically distant from any lineage described for this species complex (Haitao et al. 2007) and might correspond to an Arctic genotype. Endemism has been recently suggested for a number of Arctic protists from the Baffin Bay and the Beaufort Sea (Terrado et al. 2013). Endemic polar species include in particular the green alga Arctic *Micromonas* (Lovejoy et al. 2007), several foraminiferan species (Darling et al.

2007, Pawlowski et al. 2008), and the Antarctic terrestrial diatoms *Pinnularia borealis* Ehrenberg and *Hantzschia amphioxys* (Ehrenberg) Grunow (Souffreau et al. 2013).

Two species found here, *Porosira glacialis* and *T. gravida*, are considered to have bipolar distribution (McMinn et al. 2005, Whittaker et al. 2012, Goes et al. 2014). The presence of the same species in ecologically related but geographically distant environments, such as the Arctic and the Antarctic, has been suggested for two *Fragilariopsis* Hustedt species (Lundholm & Hasle 2008) as well as the dinoflagellate *Polarella glacialis* Montresor, Procaccini & Stoecker (Montresor et al. 2003) and the ciliate *Euplotes nobilii* Valbonesi & Luporini (Di Giuseppe et al. 2014). Polar species can hardly survive in temperate and tropical waters and the evolution of polar species is thus unlikely to arise from transport of living cells between Arctic and Antarctic waters. The presence of bipolar species could be associated with a migration occurred during the last glacial period, where colder seawater at low latitudes would have permitted the survival of cells during their transport across the globe or due to more recent transport of resting forms (Montresor et al. 2003). Such resting forms could survive tropical waters or in alternative they might have been transported across the globe via the global ocean conveyor belt or other deep cold currents.

Few (5) of the strains characterized in this study belong to species that are supposed to have a wide geographical distribution (Table 2). Molecular methods have demonstrated conspecificity in widely distributed morphospecies, as for example some *Pseudo-nitzschia* (Lelong et al. 2012) or *Skeletonema* (Kooistra et al. 2008) species. Other studies on plankton biogeography indicate that populations previously thought to make up unique cosmopolitan species are often genetically distinct and reproductively isolated (Kooistra et al. 2008, Casteleyn et al. 2010). Indeed, the northern/polar ecotype of the worldwide-considered species, *C. socialis*, has been

recently described as a distinct species, i.e., *C. gelidus,* based on physiological, morphological and molecular evidence (Degerlund et al. 2012, Huseby et al. 2012, Chamnansinp et al. 2013). Subsequently all the previous reports of *C. socialis* in Arctic waters (Booth et al. 2002, Ratkova & Wassmann 2002, Sukhanova et al. 2009), including those reported for the MALINA cruise (Balzano et al. 2012b), are likely to correspond to *C. gelidus*.

Similarly, the degree of interspecific divergence between the cosmopolitan *T. rotula* and the bipolar *T. gravida* advocates they should be treated as separate species (Whittaker et al. 2012), despite previous studies suggesting that the two morphotypes are likely to be a single species (Syvertsen 1977, Sar et al. 2011). We cannot exclude that the use of more sensitive molecular markers would allow to identify differences among geographical populations of bipolar or cosmopolitan species, as demonstrated for the cosmopolitan species *Pseudo-nitzschia pungens* (Casteleyn et al. 2010). Further analyses will be required to evaluate the slight difference here found among the 28S rRNA gene sequences of the Arctic and Antarctic strains of *Porosira glacialis*.

Therefore while some species distribution patterns seem to support the hypothesis of ubiquity (Finlay & Fenchel 2004), other species are far more restricted. The availability of validated reference sequences for arctic diatoms will facilitate the interpretation of metabarcoding data and will allow to test theories on dispersal and biogeographic patterns in protists using large scale screening of environmental samples.

REFERENCES

Aizawa, C., Tanimoto, M. & Jordan, R. W. 2005. Living diatom assemblages from North Pacific and Bering Sea surface waters during summer 1999. *Deep-Sea Res. Part II-Top. Stud. Oceanogr.* 52:2186-205.

Alverson, A. J., Jansen, R. K. & Theriot, E. C. 2007. Bridging the Rubicon: phylogenetic analysis reveals repeated colonizations of marine and fresh waters by thalassiosiroid diatoms. *Mol. Phylogenet. Evol.* 45:193-210.

Amato, A., Kooistra, W. H. C. F., Ghiron, J. H. L., Mann, D. G., Proschold, T. & Montresor, M. 2007. Reproductive isolation among sympatric cryptic species in marine diatoms. *Protist* 158:193-207.

Amato, A. & Montresor, M. 2008. Morphology, phylogeny, and sexual cycle of *Pseudo-nitzschia mannii* sp. nov. (Bacillariophyceae): a pseudo-cryptic species within the *P. pseudodelicatissima* complex. *Phycologia* 47:487-97.

Balzano, S., Gourvil, P., Siano, R., Chanoine, M., Marie, D., Lessard, S., Sarno, D. & Vaulot, D. 2012a. Diversity of cultured photosynthetic flagellates in the northeast Pacific and Arctic Oceans in summer. *Biogeosciences* 9:4553-71.

Balzano, S., Marie, D., Gourvil, P. & Vaulot, D. 2012b. Composition of the summer photosynthetic pico and nanoplankton communities in the Beaufort Sea assessed by T-RFLP and sequences of the 18S rRNA gene from flow cytometry sorted samples. *ISME J* 6:1480-98.

Balzano, S., Abs, E. & Leterme, S. C. 2015. Protist diversity along a salinity gradient in a coastal lagoon. *Aquat. Microb. Ecol.* 74:263-77.

Bérard-Therriault, L., Poulin, M. & Bossé, L. 1999. *Guide d'identification du phytoplancton marin de l'estuaire et du golfe du Saint-Laurent incluant également certains protozoaires Canadian* NRC Research Press, Ottawa, 387 pp.

Booth, B. C. & Horner, R. A. 1997. Microalgae on the Arctic Ocean Section, 1994: species abundance and biomass. *Deep-Sea Res. Part II-Top. Stud. Oceanogr.* 44:1607-22.

Booth, B. C., Larouche, P., Belanger, S., Klein, B., Amiel, D. & Mei, Z. P. 2002. Dynamics of *Chaetoceros socialis* blooms in the North Water. *Deep-Sea Res. Part II-Top. Stud. Oceanogr.* 49:5003-25.

Bosak, S., Gligora Udovic, M. & Sarno, D. 2015. Morphological study of *Chaetoceros wighamii* Brightwell (Chaetocerotaceae, Bacillariophyta) from Lake Vrana, Croatia. *Acta Bot. Croat.* 74: 233–244.

Brugel, S., Nozais, C., Poulin, M., Tremblay, J.-E., Miller, L. A., Simpson, K. G., Gratton, Y. & Demers, S. 2009. Phytoplankton biomass and production in the southeastern Beaufort Sea in autumn 2002 and 2003. *Mar. Ecol.-Prog. Ser.* 377:63-77.

Cărăus, I. 2012. *Algae of Romania. A distributional checklist of actual algae. Version 2.3 third revision.* Univ. Bacau, 809 pp.

Carmack, E. C. & MacDonald, R. W. 2002. Oceanography of the Canadian shelf of the Beaufort Sea: a setting for marine life. *Arctic* 55:29-45.

Caron, G., Michel, C. & Gosselin, M. 2004. Seasonal contributions of phytoplankton and fecal pellets to the organic carbon sinking flux in the North Water (northern Baffin Bay). *Mar. Ecol.-Prog. Ser.* 283:1-13.

Casteleyn, G., Leliaert, F., Backeljau, T., Debeer, A.-E., Kotaki, Y., Rhodes, L., Lundholm, N., Sabbe, K. & Vyverman, W. 2010. Limits to gene flow in a cosmopolitan marine planktonic diatom. *P. Natl. Acad. Sci. USA* 107:12952-57.

Chamnansinp, A., Li, Y., Lundholm, N. & Moestrup, O. 2013. Global diversity of two widespread, colony forming diatoms of the marine plankton, *Chaetoceros socialis* (syn. *C. radians*) and *Chaetoceros gelidus* sp. nov. *J. Phycol.* 49:1128-41.

Choi, H. G., Joo, H. M., Jung, W., Hong, S. S., Kang, J. S. & Kang, S. H. 2008. Morphology and phylogenetic relationships of some psychrophilic polar diatoms (Bacillariophyta). *Nova Hedwigia*:7-30.

Cleve, P. 1896. Diatoms from Baffins Bay and Davis Strait. *Kongliga Svenska Vetenskaps-Akademien* 22:1-22.

Coleman, A. W. 2001. Biogeography and speciation in the *Pandorina/Volvulina* (Chlorophyta) superclade. *J. Phycol.* 37:836-51.

Coleman, A. W. 2009. Is there a molecular key to the level of "biological species" in eukaryotes? A DNA guide. *Mol. Phylogenet. Evol.* 50:197-203.

Comeau, A. M., Li, W. K. W., Tremblay, J.-E., Carmack, E. C. & Lovejoy, C. 2011. Arctic Ocean microbial community structure before and after the 2007 record sea ice minimum. *Plos One* 6:e27492.

Coupel, P., Matsuoka, A., Ruiz-Pino, D., Gosselin, M., Marie, D., Tremblay, J.-E. & Babin, M. 2015. Pigment signatures of phytoplankton communities in the Beaufort Sea. *Biogeosciences* 12:991-1006.

Crawford, R. M., Gardner, C. & Medlin, L. K. 1994. The genus *Attheya*. I. A description of four new taxa, and the transfer of *Gonioceros septentrionalis* and *G. armatus*. *Diatom Res.* 9:27-51.

Darling, K. F., Kucera, M. & Wade, C. M. 2007. Global molecular phylogeography reveals persistent Arctic circumpolar isolation in a marine planktonic protist. *P. Natl. Acad. Sci. USA*104:5002-07.

Degerlund, M. & Eilertsen, H. C. 2010. Main species characteristics of phytoplankton spring blooms in NE Atlantic and Arctic waters (68-80°N). *Estuar. Coast.* 33:242-69.

Degerlund, M., Huseby, S., Zingone, A., Sarno, D. & Landfald, B. 2012. Functional diversity in cryptic species of *Chaetoceros socialis* Lauder (Bacillariophyceae). *J. Plankton Res.* 34:416-31.

Di Giuseppe, G., Erra, F., Frontini, F. P., Dini, F., Vallesi, A. & Luporini, P. 2014. Improved description of the bipolar ciliate, *Euplotes petzi,* and definition of its basal position in the *Euplotes* phylogenetic tree. *Eur. J. Protistol.* 50:402-11.

Dunthorn, M., Klier, J., Bunge, J. & Stoeck, T. 2012. Comparing the hyper-variable V4 and V9 regions of the small subunit rDNA for assessment of ciliate environmental diversity. *J. Eukaryot. Microbiol.* 59:185-87.

Felsenstein, J. 1985. Confidence limits on phylogenies. An approach using the bootstrap. *Evolution* 39:783-91.

Finlay, B. J. & Fenchel, T. 2004. Cosmopolitan metapopulations of free-living microbial eukaryotes. *Protist* 155:237-44.

Goes, J. I., Gothes, H. D. R., Haugen, E. M., McKee, K. T., D'Sa, E. J., Chekalyuk, A. M., Stoecker, D. K., Stabeno, P. J., Saitoh, S. & Sambrotto, R. N. 2014. Fluorescence, pigment and microscopic characterization of Bering Sea phytoplankton community structure and photosynthetic competency in the presence of a Cold Pool during summer. *Deep-Sea Res. Part II-Top. Stud. Oceanogr.* 109:84-99.

Gosselin, M., Levasseur, M., Wheeler, P. A., Horner, R. A. & Booth, B. C. 1997. New measurements of phytoplankton and ice algal production in the Arctic Ocean. *Deep-Sea Res. Part II-Top. Stud. Oceanogr.* 44:1623-44.

Gu, H., Zeng, N., Xie, Z., Wang, D., Wang, W. & Yang, W. 2013. Morphology, phylogeny, and toxicity of Atama complex (Dinophyceae) from the Chukchi Sea. *Polar Biol* 36:427-36.

Guillard, R. R. L. 1975. Culture of phytoplankton for feeding marine invertebrates. *In*: Smith, W. L. & Chanley, M. H. [Eds.] *Culture of marine invertebrate animals.* Plenum Book Publication Corporation, New York, pp. 29-60.

Guillou, L., Eikrem, W., Chretiennot-Dinet, M. J., Le Gall, F., Massana, R., Romari, K., Pedros-Alio, C. & Vaulot, D. 2004. Diversity of picoplanktonic prasinophytes assessed by direct nuclear SSU rDNA sequencing of environmental samples and novel isolates retrieved from oceanic and coastal marine ecosystems. *Protist* 155:193-214.

Guinder, V. A., Molinero, J. C., Popovich, C. A., Marcovecchio, J. E. & Sommer, U. 2012. Dominance of the planktonic diatom *Thalassiosira minima* in recent summers in the Bahía Blanca Estuary, Argentina. *J. Plankton Res.* 34:995-1000.

Guiry, M. D. 2012. How many species of algae are there? *J. Phycol.* 48:1057-63.

Guo, L., Sui, Z., Zhang, S., Ren, Y. & Liu, Y. 2015. Comparison of potential diatom 'barcode' genes (the 18S rRNA gene and ITS, COI, rbcL) and their effectiveness in discriminating and determining species taxonomy in the Bacillariophyta. *Int. J. Syst. Evol. Micr.* 65:1369-80.

Haitao, L., Guanpin, Y., Ying, S., Suihan, W. & Xiufang, Z. 2007. *Cylindrotheca closterium* is a species complex as was evidenced by the variations of rbcL gene and SSU rDNA. *Journal of Ocean University of China* 6:167-74.

Hall, T. A. 1999. BioEdit: a user-friendly biological sequence alignement editor and analysis program for Windows 95/98/NT. *Nucleic Acid symposium Series* 41:95-98.

Hällfors, G. 2004. Checklist of Baltic Sea phytoplankton species (including some heterotrophic protistan groups). *Baltic Sea Environment Proceedings* 95:1-208.

Hasle, G. R. 1964. *Nitzschia* and *Fragilariopsis* species studied in the light and electron microscopes. I. Some marine species of the group Nitzschiaella and Lanceolate. *Skrifter utgitt av Det Norske Videnskaps-Akademi i Oslo. I Matematisk-Naturvidenskapelig Klasse. Ny serie* 16:1-48.

Hasle, G. R., Medlin, L. K. & Syvertsen, E. E. 1994. *Synedropsis* gen. nov., a genus of araphid diatoms associated with sea ice. *Phycologia* 33:248-70.

Hasle, G. R. & Syvertsen, E. E. 1997. Marine diatoms. *In*: Tomas, C. R. [Ed.] *Identifying marine phytoplankton.* Academic Press, San Diego, pp. 5-385.

Hasle, G. R., Von Stosch, H. A. & Syvertsen, E. E. 1983. Cymatosiraceae, a new diatom family. *Bacillaria* 6:9-156.

Hill, V., Cota, G. & Stockwell, D. 2005. Spring and summer phytoplankton communities in the Chukchi and Eastern Beaufort Seas. *Deep-Sea Res. Part II-Top. Stud. Oceanogr.* 52:3369-85.

Hoppenrath, M., Beszteri, B., Drebes, G., Halliger, H., Van Beusekom, J. E. E., Janisch, S. & Wiltshire, K. H. 2007. *Thalassiosira* species (Bacillariophyceae, Thalassiosirales) in the North Sea at Helgoland (German bight) and Sylt (North Frisian Wadden Sea). A first approach to assessing diversity. *Eur. J. Phycol.* 42:271-88.

Horner, R. & Schrader, G. C. 1982. Relative contributions of ice algae, phytoplankton, and benthic microalgae to primary production in nearshore regions of the Beaufort Sea. *Arctic* 35:485-503.

Huseby, S., Degerlund, M., Zingone, A. & Hansen, E. 2012. Metabolic fingerprinting reveals differences between northern and southern strains of the cryptic diatom *Chaetoceros socialis*. *Eur. J. Phycol.* 47:480-89.

Jahn, R. & Kusber, W. H. 2005. Reinstatement of the genus *Ceratoneis* Ehrenberg and lectotypification of its type specimen: *C. Closterium* Ehrenberg. *Diatom Res.* 20:295-304.

Jensen, K. G. & Moestrup, Ø. 1998. The genus *Chaetoceros* (Bacillariophyceae) in inner Danish coastal waters. *Nord. J. Bot.* 18 :88

Jukes, T. H. & Cantor, C. R. 1969. Evolution of protein molecules. *In*: Munro, H. N. [Ed.] *Mammalian protein metabolism.* Academic Press, New York, pp. 21-123.

Kaczmarska, I., Beaton, M., Benoit, A. C. & Medlin, L. K. 2006. Molecular phylogeny of selected members of the order Thalassiosirales (Bacillariophyta) and evolution of the fultoportula. *J. Phycol.* 42:121-38.

Kaczmarska, I., Mather, L., Luddington, I. A., Muise, F. & Ehrman, J. 2014. Cryptic diversity in a cosmopolitan diatom known as *Asterionellopsis glacialis* (Fragilariaceae): Implications for ecology, biogeography, and taxonomy. *Am. J. Bot.* 101:267-86.

Katsuki, K., Takahashi, K., Onodera, J., Jordan, R. W. & Suto, I. 2009. Living diatoms in the vicinity of the North Pole, summer 2004. *Micropaleontology* 55:137-70.

Keller, A., Schleicher, T., Schultz, J., Muller, T., Dandekar, T. & Wolf, M. 2009. 5.8S-28S rRNA interaction and HMM-based ITS2 annotation. *Gene* 430:50-57.

Kimura, M. 1980. A simple method for estimating evolutionary rates of base substitutions through comparative studies of nucleotide sequences. *J. Mol. Evol.* 16:111-20.

Kooistra, W. H. C. F., Sarno, D., Balzano, S., Gu, H., Andersen, R. A. & Zingone, A. 2008. Global diversity and biogeography of *Skeletonema* species (Bacillariophyta). *Protist* 159:177-93.

Kooistra, W., Sarno, D., Hernandez-Becerril, D. U., Assmy, P., Di Prisco, C. & Montresor, M. 2010. Comparative molecular and morphological phylogenetic analyses of taxa in the Chaetocerotaceae (Bacillariophyta). *Phycologia* 49:471-500.

Le Gall, F., Rigaut-Jalabert, F., Marie, D., Garczarek, L., Viprey, M., Gobet, A. & Vaulot, D. 2008. Picoplankton diversity in the South-East Pacific Ocean from cultures. *Biogeosciences* 5:203-14.

Lee, M.-A., Faria, D. G., Han, M.-S., Lee, J. & Ki, J.-S. 2013. Evaluation of nuclear ribosomal RNA and chloroplast gene markers for the DNA taxonomy of centric diatoms. *Biochem. Syst. Ecol.* 50:163-74.

Lelong, A., Hégaret, H., Soudant, P. & Bates, S., S. 2012. *Pseudo-nitzschia* (Bacillariophyceae) species, domoic acid and amnesic shellfish poisoning: revisiting previous paradigms. *Phycologia* 51:168-216.

Lenaers, G., Maroteaux, L., Michot, B. & Herzog, M. 1989. Dinoflagellates in evolution. A molecular phylogenetic analysis of large subunit ribosomal RNA. *J. Mol. Evol.* 29:40-51.

Lepère, C., Demura, M., Kawachi, M., Romac, S., Probert, I. & Vaulot, D. 2011. Whole Genome Amplification (WGA) of marine photosynthetic eukaryote populations. *FEMS Microbiol. Ecol.* 76:513-23.

Lim, H. C., Teng, S. T., Leaw, C. P. & Lim, P. T. 2013. Three novel species in the *Pseudo-nitzschia pseudodelicatissima* complex: *P. batesiana* sp. nov., *P. lundholmiae* sp. nov., and *P. fukuyoi* sp. nov. (Bacillariophyceae) from the strait of Malacca, Malaysia. *J. Phycol.* 49:902-16.

Logares, R., Audic, S., Santini, S., Pernice, M. C., de Vargas, C. & Massana, R. 2012. Diversity patterns and activity of uncultured marine heterotrophic flagellates unveiled with pyrosequencing. *ISME J* 6:1823-33.

Logares, R., Audic, S., Bass, D., Bittner, L., Boutte, C., Christen, R., Claverie, J.-M., Decelle, J., Dolan, J. R., Dunthorn, M., Edvardsen, B., Gobet, A., Kooistra, W. H. C. F., Mahe, F., Not, F., Ogata, H., Pawlowski, J., Pernice, M. C., Romac, S., Shalchian-Tabrizi, K., Simon, N., Stoeck, T., Santini, S., Siano, R., Wincker, P., Zingone, A., Richards, T. A., de Vargas, C. & Massana, R. 2014. Patterns of Rare and Abundant Marine Microbial Eukaryotes. *Curr. Biol.* 24:813-21.

Lovejoy, C., Legendre, L., Martineau, M. J., Bacle, J. & von Quillfeldt, C. H. 2002. Distribution of phytoplankton and other protists in the North Water. *Deep-Sea Res. Part II-Top. Stud. Oceanogr.* 49:5027-47.

Lovejoy, C., Vincent, W. F., Bonilla, S., Roy, S., Martineau, M.-J., Terrado, R., Potvin, M., Massana, R. & Pedros-Alio, C. 2007. Distribution, phylogeny, and growth of cold-adapted picoprasinophytes in arctic seas. *J. Phycol.* 43:78-89.

Lovejoy, C. & Potvin, M. 2011. Microbial eukaryotic distribution in a dynamic Beaufort Sea and the Arctic Ocean. *J. Plankton Res.* 33:431-44.

Luddington, I. A., Kaczmarska, I. & Lovejoy, C. 2012. Distance and character-based evaluation of the V4 region of the 18S rRNA gene for the identification of Diatoms (Bacillariophyceae). *Plos One* 7:e45664.

Luddington, I. A., Lovejoy, C. & Kaczmarska, I. 2016. Species-rich meta-communities of the diatom order Thalassiosirales in the Arctic and northern Atlantic Ocean. *J. Plankton Res.* doi:10.1093/plankt/fbw030

Lundholm, N., Daugbjerg, N. & Moestrup, O. 2002. Phylogeny of the Bacillariaceae with emphasis on the genus *Pseudo-nitzschia* (Bacillariophyceae) based on partial LSU rDNA. *Eur. J. Phycol.* 37:115-34.

Lundholm, N., Moestrup, O., Hasle, G. R. & Hoef-Emden, K. 2003. A study of the *Pseudo-nitzschia pseudodelicatissima/cuspidata* complex (Bacillariophyceae): What is *P. pseudodelicatissima*? *J. Phycol.* 39:797-813.

Lundholm, N., Moestrup, O., Kotaki, Y., Hoef-Emden, K., Scholin, C. & Miller, P. 2006. Inter- and intraspecific variation of the *Pseudo-nitzschia delicatissima* complex

(Bacillariophyceae) illustrated by rRNA probes, morphological data and phylogenetic analyses. *J. Phycol.* 42:464-81.

Lundholm, N. & Hasle, G. R. 2008. Are *Fragilariopsis cylindrus* and *Fragilariopsis nana* bipolar diatoms? Morphological and molecular analyses of two sympatric species. *Nova Hedwigia*: 231-50.

Lundholm, N., Bates, S. S., Baugh, K. A., Bill, B. D., Connell, L. B., Leger, C. & Trainer, V. L. 2012. Cryptic and pseudo-cryptic diversity in diatoms with description of *Pseudo-nitzschia hasleana* sp. nov. and *P. fryxelliana* sp. nov. *J. Phycol.* 48:436-54.

Majaneva, M., Rintala, J. M., Piisila, M., Fewer, D. P. & Blomster, J. 2012. Comparison of wintertime eukaryotic community from sea ice and open water in the Baltic Sea, based on sequencing of the 18S rRNA gene. *Polar Biol.* 35:875-89.

Mann, D. G. & Vanormelingen, P. 2013. An Inordinate Fondness? The number, distributions, and origins of diatom species. *J. Eukaryot. Microbiol.* 60:414-20.

Marchetti, A., Lundholm, N., Kotaki, Y., Hubbard, K., Harrison, P. J. & Armbrust, E. V. 2008. Identification and assessment of domoic acid production in oceanic *Pseudo-nitzschia* (Bacillariophyceae) from iron-limited waters in the northeast subarctic pacific. *J. Phycol.* 44:650-661.

Mathews, D. H., Disney, M. D., Childs, J. L., Schroeder, S. J., Zuker, M. & Turner, D. H. 2004. Incorporating chemical modification constraints into a dynamic programming algorithm for prediction of RNA secondary structure. *P. Natl. Sci. USA* 101:7287-92.

McMinn, A., Pankowski, A. & Delfatti, T. 2005. Effect of hyperoxia on the growth and photosynthesis of polar sea ice microalgae. *J. Phycol.* 41:732-41.

McNeill, J., Barrie, F. R., Buck, W. R., Demoulin, V., Greuter, W., Hawksworth, D. L., Herendeen, P. S., Knapp, S., Marhold, K., Prado, J., Prud'homme van Reine, W. F., Smith, G. F., Wiersema, J. H. & Turland, N. J. 2012. *International Code of Nomenclature for Algae, Fungi, and Plants (Melbourne Code) adopted by the Eighteenth International Botanical Congress Melbourne, Australia, July 2011.* Koeltz Scientific Books, Königstein. 208 pp.

Merget, B., Koetschan, C., Hackl, T., Forster, F., Dandekar, T., Muller, T., Schultz, J. & Wolf, M. 2012. The ITS2 Database*.: JoVE* 61:e3806.

Mikheyev, A. S. & Tin, M. M. Y. 2014. A first look at the Oxford Nanopore MinION sequencer. *Mol. Ecol. Resour.* 14:1097-102.

Moniz, M. B. J. & Kaczmarska, I. 2010. Barcoding of Diatoms: Nuclear encoded ITS revisited. *Protist* 161:7-34.

Montresor, M., Lovejoy, C., Orsini, L., Procaccini, G. & Roy, S. 2003. Bipolar distribution of the cyst-forming dinoflagellate *Polarella glacialis. Polar Biol.* 26:186-94.

Nanjappa, D., Kooistra, W. H. C. F. & Zingone, A. 2013. A reappraisal of the genus *Leptocylindrus* (Bacillariophyta), with the addition of three species and the erection of *Tenuicylindrus* gen. nov. *J. Phycol.* 49:917-36.

Nei, M. & Kumar, S. 2000. *Molecular Evolution and Phylogenetics.* Oxford University Press, New York, 352 pp.

Olli, K., Riser, C. W., Wassmann, P., Ratkova, T., Arashkevich, E. & Pasternak, A. 2002. Seasonal variation in vertical flux of biogenic matter in the marginal ice zone and the central Barents Sea. *J. Mar. Syst.* 38:189-204.

Orive, E., Perez-Aicua, L., David, H., Garcia-Etxebarria, K., Laza-Martinez, A., Seoane, S. & Miguel, I. 2013. The genus *Pseudo-nitzschia* (Bacillariophyceae) in a temperate estuary

with description of two new species: *Pseudo-nitzschia plurisecta* sp. nov. and *Pseudo-nitzschia abrensis* sp. nov. *J. Phycol.* 49:1192-206.

Orsini, L., Sarno, D., Procaccini, G., Poletti, R., Dahlmann, J. & Montresor, M. 2002. Toxic *Pseudo-nitzschia multistriata* (Bacillariophyceae) from the Gulf of Naples: morphology, toxin analysis and phylogenetic relationships with other *Pseudo-nitzschia* species. *Eur. J. Phycol.* 37:247-57.

Pawlowski, J., Majewski, W., Longet, D., Guiard, J., Cedhagen, T., Gooday, A. J., Korsun, S., Habura, A. A. & Bowser, S. S. 2008. Genetic differentiation between Arctic and Antarctic monothalamous foraminiferans. *Polar Biol.* 31:1205-16.

Percopo, I., Siano, R., Cerino, F., Sarno, D. & Zingone, A. 2011. Phytoplankton diversity during the spring bloom in the northwestern Mediterranean Sea. *Bot. Mar.* 54:243-67.

Percopo, I., Ruggiero, M. V., Balzano, S., Gourvil, P., Lundholm, N., Siano, R., Vaulot, D. & Sarno, D. 2016. *P. arctica* sp. nov., a new cold-water cryptic *Pseudo-nitzschia* species within the *P. pseudodelicatissima* complex. *J. Phycol.* 52:184-99.

Pickart, R. S., Schulze, L. M., Moore, G. W. K., Charette, M. A., Arrigo, K. R., van Dijken, G. & Danielson, S. L. 2013. Long-term trends of upwelling and impacts on primary productivity in the Alaskan Beaufort Sea. *Deep-Sea Res. Pt I* 79:106-21.

Ratkova, T. N. & Wassmann, P. 2002. Seasonal variation and spatial distribution of phyto- and protozooplankton in the central Barents Sea. *J. Mar. Syst.* 38:47-75.

Rimet, F., Kermarrec, L., Bouchez, A., Hoffmann, L., Ector, L. & Medlin, L. K. 2011. Molecular phylogeny of the family Bacillariaceae based on 18S rDNA sequences: focus on freshwater *Nitzschia* of the section Lanceolatae. *Diatom Res.* 26:273-91.

Rines, J. E. B. & Hargraves, P. E. 1988. *The Chaetoceros Ehrenberg (Bacillariophyceae). Flora of Narraganset Bay, Rhode Island, U.S.A.* Lubrecht & Cramer Ltd, Berlin. 196 pp.

Sar, E. A., Sunesen, I. s., Lavigne, A. S. & Lofeudo, S. 2011. *Thalassiosira rotula*, a heterotypic synonym of *Thalassiosira gravida*: morphological evidence. *Diatom Res.* 26:109-19.

Sarno, D., Kooistra, W., Medlin, L. K., Percopo, I. & Zingone, A. 2005. Diversity in the genus *Skeletonema* (Bacillariophyceae). II. An assessment of the taxonomy of *S. costatum*-like species with the description of four new species. *J. Phycol.* 41:151-76.

Sarno, D., Kooistra, W., Balzano, S., Hargraves, P. E. & Zingone, A. 2007. Diversity in the genus *Skeletonema* (Bacillariophyceae): III. Phylogenetic position and morphological variability of *Skeletonema costatum* and *Skeletonema grevillei*, with the description of *Skeletonema ardens* sp. nov. *J. Phycol.* 43:156-70.

Schloss, P. D., Jenior, M. L., Koumpouras, C. C., Westcott, S. L. & Highlander, S. K. 2016. Sequencing 16S rRNA gene fragments using the PacBio SMRT DNA sequencing system. *Peer J.* 4:e1869.

Schütt, F. 1895. Arten von *Chaetoceras* und *Peragallia. Ein Beitrag zur Hochseeflora. Berichte der Deutsche Botanisch Gesellschaft* 13:35-50.

Sherr, E. B., Sherr, B. F., Wheeler, P. A. & Thompson, K. 2003. Temporal and spatial variation in stocks of autotrophic and heterotrophic microbes in the upper water column of the central Arctic Ocean. *Deep-Sea Res. Pt I* 50:557-71.

Sorhannus, U. & Fox, M. G. 2012. Phylogenetic analyses of a combined data set suggest that the *Attheya* lineage is the closest living relative of the pennate diatoms (Bacillariophyceae). *Protist* 163:252-62.

Sorhannus, U., Ortiz, J. D., Wolf, M. & Fox, M. G. 2010. Microevolution and speciation in *Thalassiosira weissflogii* (Bacillariophyta). *Protist* 161:237-49.

Souffreau, C., Vanormelingen, P., Van de Vijver, B., Isheva, T., Verleyen, E., Sabbe, K. & Vyverman, W. 2013. Molecular evidence for distinct Antarctic lineages in the cosmopolitan terrestrial diatoms *Pinnularia borealis* and *Hantzschia amphioxys*. *Protist* 164:101-15.

Stoeck, T., Bass, D., Nebel, M., Christen, R., Jones, M. D. M., Breiner, H. W. & Richards, T. A. 2010. Multiple marker parallel tag environmental DNA sequencing reveals a highly complex eukaryotic community in marine anoxic water. *Mol. Ecol.* 19:21-31.

Stonik, I. V., Orlova, T. Y. & Crawford, R. M. 2006. *Attheya ussurensis* sp. nov. (Bacillariophyta) -a new marine diatom from the coastal waters of the Sea of Japan and a reappraisal of the genus. *Phycologia* 45:141-147.

Sukhanova, I. N., Flint, M. V., Pautova, L. A., Stockwell, D. A., Grebmeier, J. M. & Sergeeva, V. M. 2009. Phytoplankton of the western Arctic in the spring and summer of 2002: Structure and seasonal changes. *Deep-Sea Res. Part II-Top. Stud. Oceanogr.* 56:1223-36.

Syvertsen, E. E. 1977. *Thalassiosira rotula* and *T. gravida*: ecology and morphology. *Beiheft zur Nova Hedwigia* 54:99-112.

Syvertsen, E. E. 1986. *Thalassiosira hispida* sp. nov., a marine planktonic diatom. In: M. Ricard [Ed.] *Proceedings of the Eighth International Diatom Symposium*, Koeltz, Koenigstein, pp. 33-42.

Syvertsen, E. E. & Hasle, G. R. 1983. The diatom genus *Eucampia*: morphology and taxonomy. *Bacillaria* 6:169-210.Tamura, K. & Nei, M. 1993. Estimation of the number of nucleotide substitutions in the control region of mitochondrial DNA in humans and chimpanzees. *Mol. Biol. Evol.* 10:512-26.

Tamura, K., Peterson, D., Peterson, N., Stecher, G., Nei, M. & Kumar, S. 2011. MEGA5: molecular evolutionary genetics analysis using maximum likelihood, evolutionary distance, and maximum parsimony methods. *Mol. Biol. Evol.* 28:2731-39.

Terrado, R., Scarcella, K., Thaler, M., Vincent, W. F. & Lovejoy, C. 2013. Small phytoplankton in Arctic seas: vulnerability to climate change. *Biodiversity* 14:2-18.

Tschochner, H. & Hurt, E. 2003. Pre-ribosomes on the road from the nucleolus to the cytoplasm. *Trends Cell Biol.* 13:255-63.

Tuschling, K., von Juterzenka, K., Okolodkov, Y. B. & Anoshkin, A. 2000. Composition and distribution of the pelagic and sympagic algal assemblages in the Laptev Sea during autumnal freeze-up. *J. Plankton Res.* 22:843-64.

von Quillfeldt, C. H. 2000. Common diatom species in arctic spring blooms: Their distribution and abundance. *Bot. Mar.* 43:499-516.

von Quillfeldt, C. H., Ambrose, W. G. & Clough, L. M. 2003. High number of diatom species in first-year ice from the Chukchi Sea. *Polar Biol.* 26:806-18.

Wang, J., Cota, G. F. & Comiso, J. C. 2005. Phytoplankton in the Beaufort and Chukchi Seas: Distribution, dynamics, and environmental forcing. *Deep-Sea Res. Part II-Top. Stud. Oceanogr.* 52:3355-68.

Whittaker, K. A., Rignanese, D. R., Olson, R. J. & Rynearson, T. A. 2012. Molecular subdivision of the marine diatom *Thalassiosira rotula* in relation to geographic distribution, genome size, and physiology. *Bmc Evolutionary Biology* 12. doi**:** 10.1186/1471-2148-12-209

Wolf, M., Achtziger, M., Schultz, J., Dandekar, T. & Muller, T. 2005. Homology modeling revealed more than 20,000 rRNA internal transcribed spacer 2 (ITS2) secondary structures. *Rna-a Publication of the Rna Society* 11:1616-23.

Zhu, F., Massana, R., Not, F., Marie, D. & Vaulot, D. 2005. Mapping of picoeucaryotes in marine ecosystems with quantitative PCR of the 18S rRNA gene. *Fems Microbiol. Ecol.* 52:79-92.

Table 1. List of the strain isolated during the MALINA cruise and used in the present study.

Family	Species	Strain code[1]	Isolation site[2]		Morphology[3]	Genbank accession numbers[4]		
			Station	Depth (m)		18S	28S	ITS
Bacillariaceae	*Cylindrotheca closterium*	RCC1985	280	30	LM, TEM	JF794039	JQ995403	
	Nitzschia pellucida	RCC2276	BEA130709A	0	LM,TEM	JF794052	JQ995450	
	Pseudo-nitzschia granii	RCC2006	PAC080709A	5	LM, TEM		JQ995420	
	Pseudo-nitzschia granii	RCC2008	PAC080709A	5	LM	JN934671	JQ995421	
	Pseudo-nitzschia granii	RCC2273	PAC060709A	0			JQ995391	
	Pseudo-nitzschia arctica	RCC2002	690	29	LM, TEM, SEM		JQ995416	
	Pseudo-nitzschia arctica	RCC2004	690	29	LM, TEM, SEM	JF794046	JQ995418	
	Pseudo-nitzschia arctica	RCC2005	690	29	LM, TEM		JQ995419	
	Pseudo-nitzschia arctica	RCC2517	690	29	LM, TEM, SEM		JQ995461	
Fragilariaceae	*Synedropsis hyperborea*	RCC2043	280	30	LM, TEM, SEM	JF794051	JQ995434	
	Synedropsis hyperborea	RCC2520	280	30	LM		JQ995463	
Attheyaceae	*Attheya septentrionalis*	RCC1986	280	30	LM, TEM, SEM	JF794040	JQ995404	
	Attheya septentrionalis	RCC1988	280	30	LM		JQ995405	
	Attheya septentrionalis	RCC2042	680	3	LM	JN934675	JQ995433	
Thalassiosiraceae	*Thalassiosira gravida*	RCC1984	280	30	LM	JN934669	JQ995402	
	Thalassiosira gravida	RCC1999	280	30	LM, TEM, SEM		JQ995414	
	Thalassiosira cf. *hispida*	RCC2521	680	40	TEM, SEM	JN934691	JQ995464	
	Thalassiosira minima	RCC2265	394	3	LM, TEM, SEM	JN934676	JQ995440	
	Thalassiosira minima	RCC2266	394	3	LM, TEM, SEM		JQ995441	
	Thalassiosira minima	RCC2269	PAC050709A	0	LM, TEM, SEM		JQ995444	
	Thalassiosira nordenskioeldii	RCC2000	690	29	LM, TEM, SEM	JF794045	JQ995415	
	Thalassiosira nordenskioeldii	RCC2021	680	3	LM, TEM, SEM		JQ995428	
	Thalassiosira nordenskioeldii	RCC2522	620	3	LM			
	Porosira glacialis	RCC1995	690	29	LM, SEM, TEM			
	Porosira glacialis	RCC2039	690	29	LM	JN934673	JQ995432	

	Shionodiscus bioculatus	RCC1991	620	65	LM, TEM, SEM	JF794041	JQ995408
Cymatosiraceae	*Arcocellulus cornucervis*	RCC2270	ARC120709A	0	LM, SEM,TEM	JN934677	JQ995445
Hemiaulaceae	*Eucampia groenlandica*	RCC1996	690	29	LM, TEM, SEM	JF794043	JQ995412
	Eucampia groenlandica	RCC2037	690	29	LM, SEM		JQ995430
	Eucampia groenlandica	RCC2038	690	29	LM, SEM		JQ995431
Chaetoceraceae	*Chaetoceros decipiens*	RCC1997	690	29	LM, TEM, SEM	JF794044	JQ995413
	Chaetoceros gelidus	RCC1990	620	65	LM		JQ995407
	Chaetoceros gelidus	RCC1992	620	65	LM, TEM, SEM	JF794042	JQ995409
	Chaetoceros gelidus	RCC1994	690	29	LM, SEM		JQ995411
	Chaetoceros gelidus	RCC2046	280	30	LM		JQ995435
	Chaetoceros gelidus	RCC2271	690	3	LM,SEM		JQ995446
	Chaetoceros gelidus	MALINA E65 PG4	690	29			JQ995393
	Chaetoceros gelidus	MALINA E65 PG18	690	29			
	Chaetoceros gelidus	MALINA S135	BEA140709A	0			JQ995396
	Chaetoceros neogracilis clade I	RCC2003	690	29	LM		JQ995417	KT860511
	Chaetoceros neogracilis clade I	RCC2011	620	3	LM		JQ995423	KT860513
	Chaetoceros neogracilis clade I	RCC2017	760	3	LM, TEM		JQ995427	KT860517
	Chaetoceros neogracilis clade I	RCC2262	460	3	LM		JQ995437	KT860520
	Chaetoceros neogracilis clade I	RCC2263	235	3	LM		JQ995438	KT860521
	Chaetoceros neogracilis clade I	RCC2264	235	3	LM		JQ995439	KT860522
	Chaetoceros neogracilis clade I	RCC2267	394	3			JQ995442	KT860523
	Chaetoceros neogracilis clade I	RCC2274	620	3	LM		JQ995448	KT860526
	Chaetoceros neogracilis clade I	RCC2275	620	3	LM		JQ995449	KT860527
	Chaetoceros neogracilis clade I	RCC2278	320	3	LM		JQ995452	KT860529
	Chaetoceros neogracilis clade I	RCC2279	320	3	LM		JQ995453	KT860530
	Chaetoceros neogracilis clade I	RCC2280	760	3	LM		JQ995454	KT860531
	Chaetoceros neogracilis clade I	RCC2281	760	3	LM		JQ995455	KT860532
	Chaetoceros neogracilis clade I	RCC2507	235	25	LM		JQ995459	KT860536
	Chaetoceros neogracilis clade I	MALINA S441 P21-E6	320	3			JQ995397	KT860541
	Chaetoceros neogracilis clade I	MALINA S502 P27.B3	760	3			JQ995399	KT860540
	Chaetoceros neogracilis clade I	MALINA S509	760	3			KT884482	KT884482

Chaetoceros neogracilis clade I	MALINA S510	760	3			KT884483	KT884483
Chaetoceros neogracilis clade I	MALINA S511	760	3			KT884484	KT884484
Chaetoceros neogracilis clade I	MALINA S512	760	3			KT884485	KT884485
Chaetoceros neogracilis clade II	RCC2261	460	3	LM		JQ995436	KT860519
Chaetoceros neogracilis clade II	RCC2268	BEA130709A	0	LM		JQ995443	KT860524
Chaetoceros neogracilis clade II	RCC2272	BEA130709A	0	LM,SEM		JQ995447	KT860525
Chaetoceros neogracilis clade II	RCC2277	BEA130709A	0	LM		JQ995451	KT860528
Chaetoceros neogracilis clade II	RCC2282	760	3	LM		JQ995456	KT860533
Chaetoceros neogracilis clade II	RCC2318	620	65	LM	JN934684	JQ995457	KT860534
Chaetoceros neogracilis clade II	RCC2506	235	3	LM		JQ995458	KT860535
Chaetoceros neogracilis clade II	MALINA E43.N2	BEA140709A	0			JQ995392	
Chaetoceros neogracilis clade III	RCC1989	620	65	LM		JQ995406	KT860509
Chaetoceros neogracilis clade III	RCC1993	620	65	LM		JQ995410	KT860510
Chaetoceros neogracilis clade IV	RCC2010	620	3	LM, SEM		JQ995422	KT860512
Chaetoceros neogracilis clade IV	RCC2012	110	3	LM, SEM,TEM		JQ995424	KT860514
Chaetoceros neogracilis clade IV	RCC2014	110	3	LM, TEM		JQ995425	KT860515
Chaetoceros neogracilis clade IV	RCC2016	760	3	LM, SEM	JF794049	JQ995426	KT860516
Chaetoceros neogracilis clade IV	RCC2022	680	3	LM, SEM		JQ995429	KT860518
Chaetoceros neogracilis clade IV	MALINA FT56.6 PG6	110	3			JQ995395	KT860542

[1] RCC: Roscoff culture collection. More information on the strains is available at http://roscoff-culture-collection.org/. Strains without an RCC code are no longer available.

[2] Sampling location of the MALINA cruise. See Table S1 for more details

[3] Technique used for the morphological identification: LM, Light Microscopy; TEM, Transmission Electron Microscopy; SEM, Scanning Electron Microscopy.

[4] Please note that the V4 region of the 18S rRNA gene has been sequenced from all the strains.

Table 2. Geographic distribution and morphological references of the species identified in the present study.

Species	Morphological references	Global distribution	Distribution in Arctic waters
Cylindrotheca closterium (Ehrenberg) Lewin & Reimann	Hasle & Syvertsen 1997, and references therein Jahn & Kusber 2005	Cosmopolitan (Hasle & Syvertsen 1997) Common in Arctic waters	Beaufort Sea (Horner & Schrader 1982) Chukchi Sea (von Quillfeldt 2000) White and Barents Sea (Luddington et al. 2016) Laptev Sea (Tuschling et al. 2000) Central Arctic Ocean (Katsuki et al. 2009)
Nitzschia pellucida Grunow	Bérard-Therriault et al. 1999, and references therein	Northern cold water region (Bérard-Therriault et al. 1999) Antarctica (Hällfors 2004) European freshwater environments (Cărăus 2012) Ishigaki Island, Japan (Lundholm et al. 2002)	Chukchi Sea (von Quillfeldt 2000)
Pseudo-nitzschia granii (Hasle) Hasle	Hasle & Syvertsen 1997, and references therein Marchetti et al. 2008	Northern cold water region to temperate? (Hasle & Syvertsen 1997) Northern Atlantic (Hasle 1964) Subarctic Pacific (Marchetti et al. 2008, this study)	Norwegian Sea (Hasle 1964) Chukchi Sea (von Quillfeldt et al. 2003) White and Barents Seas (Luddington et al. 2016)
Pseudo-nitzschia arctica Percopo & Sarno	Percopo et al. 2016	Recently described from Arctic waters (Percopo et al. 2016)	Beaufort Sea, Barrow Strait, Baffin Bay (Percopo et al. 2016)
Synedropsis hyperborea (Grunow) Hasle, Medlin & Syvertsen	Hasle et al. 1994	Northern cold water region (Hasle & Syvertsen 1997) Common in Arctic waters (Hasle et al. 1994)	Frobisher Bay, Greenland, Barents Sea (Hasle et al. 1994) Chukchi Sea (von Quillfeldt et al. 2003)
Attheya septentrionalis (Østrup) Crawford	Crawford et al. 1994 Stonik et al. 2006	Northern cold water region to temperate (Hasle & Syvertsen 1997)	Nansen Basin (Gosselin et al. 1997) Chukchi Sea (von Quillfeldt et al.

		Common in Arctic waters	2003) Baffin Bay (Caron et al. 2004) White and Barents Sea (Luddington et al. 2016) Laptev Sea (Tuschling et al. 2000)
Thalassiosira gravida Cleve	Syvertsen 1977	Northern and southern cold water regions (Whittaker et al. 2012) Common in Arctic waters	Nansen Basin, Chukchi Sea (Gosselin et al. 1997) Baffin Bay (Lovejoy et al. 2002) Laptev Sea (Tuschling et al. 2000) Central Arctic Ocean (Katsuki et al. 2009)
Thalassiosira cf. *hispida* Syvertsen	Syvertsen 1986	Northern cold water region to temperate (Hasle & Syvertsen 1997)	Amundsen Gulf (Luddington et al. 2016) Central Arctic Ocean (Katsuki et al. 2009) Svalbard and the Barents Sea (von Quillfeldt 2000) Chukchi Sea (von Quillfeldt et al. 2003)
Thalassiosira minima Gaarder	Hasle & Syvertsen 1997, and references therein Hoppenrath et al. 2007	Cosmopolitan excluding polar regions (Hasle & Syvertsen 1997) North Sea (Hoppenrath et al. 2007) North Atlantic Ocean (Luddington et al. 2016, as *T*. aff. *minima*) Warm waters in coastal and estuarine systems (Guinder et al. 2012)	First report in this study
Thalassiosira nordenskioeldii Cleve	Hasle & Syvertsen 1997, and references therein	Northern cold water region to temperate (Hasle & Syvertsen 1997) Common in Arctic waters	Amundsen Gulf (Luddington et al. 2016) Canadian Arctic (Aizawa et al. 2005) Baffin Bay (Caron et al. 2004) Barents Sea (Degerlund & Eilertsen 2010) Laptev Sea (Tuschling et al. 2000)

			Chukchi Sea (von Quillfeldt et al. 2003)
			Central Arctic Ocean (Katsuki et al. 2009)
Porosira glacialis (Grunow) Jørgensen	Hasle & Syvertsen 1997, and references therein	Northern cold water region to temperate, southern cold water region (Hasle & Syvertsen 1997) Common in Arctic waters	Amundsen Gulf (Luddington et al. 2016) Chukchi Sea (Gosselin et al. 1997) Beaufort Sea (Sukhanova et al. 2009) White and Barents Seas (Olli et al. 2002) Central Arctic Ocean (Katsuki et al. 2009)
Shionodiscus bioculatus (Grunow) Alverson, Kang & Theriot	as *Thalassiosira bioculata*: Hasle & Syvertsen 1997, and references therein Bérard-Therriault et al. 1999, and references therein	Northern cold water region (Hasle & Syvertsen 1997) Common in Arctic waters	Amundsen Gulf (Luddington et al. 2016) Chukchi Sea (von Quillfeldt et al. 2003) White and Barents Sea (Luddington et al. 2016) Norwegian coastal waters (Degerlund & Eilertsen 2010) Baffin Bay (Booth et al. 2002) Central Arctic Ocean (Katsuki et al. 2009)
Arcocellulus cornucervis Hasle, von Stosch & Syvertsen	Hasle et al. 1983	Northern cold and temperate waters, New Zealand (Hasle & Syvertsen 1997) Mediterranean Sea (Percopo et al. 2011)	Baffin Bay (Lovejoy et al. 2002)
Eucampia groenlandica Cleve	Syvertsen & Hasle 1983	Northern cold water region (Hasle & Syvertsen 1997) Common in Arctic waters	Baffin Bay (Cleve 1896) Laptev Sea (Tuschling et al. 2000) Barents Sea (Luddington et al. 2016)
Chaetoceros decipiens Cleve	Hasle & Syvertsen 1997, and references therein Jensen & Moestrup 1998	Cosmopolitan (Hasle & Syvertsen 1997) Common in Arctic waters	North Pacific and Bering Sea (Aizawa et al. 2005) Baffin Bay (Caron et al. 2004) Barents Sea (Ratkova & Wassmann

			2002) Norwegian coastal waters (Degerlund & Eilertsen 2010)
Chaetoceros gelidus Chamnansinp, Li, Lundholm & Moestrup	Chamnansinp et al. 2013	Northern cold water region (Chamnansinp et al. 2013)	Barents Sea, Norwegian Sea, Greenland (Chamnansinp et al. 2013)
Chaetoceros neogracilis (Schütt) VanLandingham	Schütt 1895 (as *C. gracile*) See discussion	Baltic Sea (Hällfors 2004, Majaneva et al. 2012)	Svalbard (Choi et al. 2008) Beaufort Sea (Lovejoy & Potvin 2011)

FIGURE LEGEND

Figure 1. Full 18S rRNA phylogenetic tree derived from Maximum Likelihood (ML) analysis. The tree includes at least one sequence from each genotype found within the diatom strains isolated during the MALINA cruise. Four sequences from radial centrics (*Corethron hystrix*, *Corethron pennatum*, *Rhizosolenia setigera,* and *Rhizosolenia similoides*) have been used as outgroup. The MALINA strains sequenced here are labelled in bold whereas other strains isolated from Arctic waters are underlined. The Genbank accession number is indicated next to the strain code. The percentage of replicate trees in which the associated taxa clustered together in the bootstrap test (1,000 replicates) are shown next to the branches from left (ML) to right (Neighbour-joining). Missing percentage values and "_" indicate that bootstrap values < 50 % were obtained for the corresponding node. Asterisks indicate strains isolated from the North Pacific Ocean.

Figure 2. 28S rRNA phylogenetic tree inferred by maximum likelihood (ML) analysis for the (**A**) pennate and (**B**) centric diatoms isolated during the MALINA cruise. The MALINA strains sequenced here are labelled in bold whereas other strains isolated from Arctic waters are underlined. The evolutionary histories were inferred using maximum likelihood. The percentage of trees in which the associated taxa cluster together is shown next to the branches based on Maximum Likelihood (left) and Neighbour joining (right). ML and NJ values are indicated next to the branch nodes as described in Fig. 1. Asterisks indicate strains isolated from the North Pacific Ocean.

Figure 3. 28S rRNA (**A**), ITS-1 (**B**), and 5.8S+ITS-2 (**C**) phylogenetic trees for the strains of *Chaetoceros neogracilis* strains isolated from the Beaufort Sea. For the 28S, *C. gelidus* was used to root the phylogenetic tree whereas for the ITS-1 and 5.8S + ITS-2 trees, the Antarctic strains of *Chaetoceros* sp. (CCMP187, CCMP189, CCMP190) were used as outgroup. The bootstrap values are indicated next to the branches as for Figure 1.

Figure 4. (A) *Cylindrotheca closterium*: TEM micrograph, RCC1985. Detail of the valve in which is visible the raphe interruption. Scale bar, 2 µm. (B-D) *Nitzschia pellucida*: (B) TEM micrograph, RCC2276. Whole valve. Scale bar, 5 µm. (C) TEM micrograph, RCC2276. Detail of the valve. Note the central larger interspace. Scale bar, 2 µm. (D) TEM micrograph, RCC2276. Detail of cell apex. Scale bar, 2 µm. (E-G) *Pseudo-nitzschia granii*: (E) TEM micrograph, RCC2006. Whole valve. Scale bar, 5 µm. (F) TEM micrograph, RCC2006. Detail of the valve. Note the few incomplete poroids (arrows). Scale bar, 0.5 µm. (G) TEM micrograph, RCC2006. Detail of the valve with scattered complete poroids. Scale bar, 1 µm. (H-I) *Pseudo-nitzschia arctica*: (H) LM micrograph, RCC2002. A colony of two cells in girdle view. Scale bar, 20 µm. (I) TEM micrograph, RCC2004. Detail of the valve. Note the central larger interspace. Scale bar, 1µm. (J-N) *Synedropsis hyperborea*: (J) LM micrograph, RCC2043. Cell in valve view. Scale bar, 2µm. (K) SEM micrograph, RCC2043. External view of the central part of the valve. Scale bar, 1 µm. (L) SEM micrograph, RCC2043. Internal view of the apex. Note apical slit field and rimoportula. Scale bar, 0.1 µm. (M) SEM micrograph, RCC2043. External view of the apex. Note apical slit field and absence of rimoportula. Scale bar, 0.5 µm. (N) SEM micrograph, RCC2043. External view of the apex. Note apical slit field and rimoportula. Scale bar, 0.2 µm.

Figure 5. (A-E) *Attheya septentrionalis*: (A) LM micrograph, RCC1986. Cells in girdle view. Scale bar, 10 μm. (B) LM micrograph, RCC2042. A cell in girdle view. Scale bar, 20 μm. (C) TEM micrograph, RCC1986. A circular valve. Scale bar, 1 μm. (D) TEM micrograph, RCC2042. A horn with three longitudinal strips. Scale bar, 0.5 μm. (E) TEM micrograph, RCC1986. A horn with four longitudinal strips. Scale bar, 0.5 μm. (F-G) *Thalassiosira gravida*: (F) LM micrograph, RCC1999. Three cells joined in colony. Scale bar, 20 μm. (G) TEM micrograph, RCC1999. A valve with the central cluster of fultoportulae and several fultoportulae scattered on the valve face. Scale bar, 5 μm. (H-K) *Thalassiosira* cf. *hispida*: (H) SEM micrograph, RCC2521. A cell in valve view with a ring of marginal fultoportulae and one central fultoportula. Note the rimoportula between two marginal fultoportulae. Scale bar, 1 μm. (I) TEM micrograph, RCC2521. Detail of a valve; short and minute spines are present on the hyaline margin and in the areolae foramina. Scale bar, 1 μm. (J) SEM micrograph, RCC2521. The girdle composed by the valvocopula, a copula and open bands. Scale bar, 1 μm. (K) TEM micrograph, RCC2521. Detail of the fultoportula. Scale bar, 0.2 μm. (L-P) *Thalassiosira minima*: (L) LM micrograph, RCC2269. Cell in girdle view with two chloroplasts. Scale bar, 2 μm. (M) SEM micrograph, RCC2266. External view of the valve with a ring of marginal fultoportulae and two central fultoportulae. Note the rimoportula between two marginal fultoportulae. Scale bar, 1 μm. (N) SEM micrograph, RCC2269. Internal view of a valve. Scale bar, 1 μm. (O) TEM micrograph, RCC2266. Five central fultoportulae. Scale bar, 1 μm. (P) SEM micrograph, RCC2266. Detail of two marginal fultoportulae with the small external labiate-shaped protrusions on the external face of the valve. Scale bar, 1 μm.

Figure 6. (A-C) *Thalassiosira nordenskioeldii*: (A) LM micrograph, RCC2000. A colony in girdle view. Scale bar, 5 µm. (B) TEM micrograph, RCC2000. A valve with a marginal ring of fultoportulae, one central fultoportula and one rimoportula positioned within two marginal fultoportulae. Scale bar, 2 µm. (C) SEM micrograph, RCC2000. A cell with ring of fultoportulae with long external tubes bearing a terminal collar. Scale bar, 1 µm. (D-F) *Porosira glacialis*: (D) LM micrograph, RCC1995. Cell in girdle view. Scale bar, 10 µm. (E) LM micrograph, RCC1995. Cell in valve view. Scale bar, 10 µm. (F) TEM micrograph, RCC1995. A valve with numerous fultoportulae scattered over the valve surface. Note the central annulus and the marginal rimoportula (arrow). Scale bar, 10 µm. (G-I) *Shionodiscus bioculatus*: (G) LM micrograph, RCC1991. A cell in girdle view. Scale bar, 20 µm. (H) SEM micrograph, RCC1991. External view of a cell; note the marginal ring of fultoportulae, the single fultoportula in the valve centre and a subcentral rimoportula. Scale bar, 10 µm. (I) TEM micrograph, RCC1991. Whole valve. Scale bar, 10 µm. (J-L) *Arcocellulus cornucervis*: (J) SEM micrograph, RCC2270. A slightly curved cell in girdle view. Note the conspicuous branches of the pili (arrow). Scale bar, 1 µm. (K) SEM micrograph, RCC2270. A pili valve (left) and a process valve (right). Note the ocelluli (arrows). Scale bar, 1 µm. (L) A pili valve in which the short spinules are visible near the pilus base (arrows). Scale bar, 2 µm.

Figure 7. (A) *Arcocellulus cornucervis*: TEM micrograph, RCC2270. A process valve in which the two ocelluli are visible (arrows). Scale bar, 1 µm. (B-C) *Eucampia groenlandica*: (B) LM micrograph, RCC2037. Part of a colony. Scale bar, 5 µm (C) SEM micrograph, RCC2037. A valve with the central rimoportula (arrow). Scale bar, 1 µm. (D-I) *Chaetoceros decipiens*: (D) LM micrograph, RCC1997. Part of a colony. Scale bar, 20µm. (E) LM micrograph, RCC1997. A

solitary cell. Scale bar, 20 μm. (F) TEM micrograph, RCC1997. A terminal valve. Scale bar, 5 μm. (G) SEM micrograph, RCC1997. Two intercalary valves. Scale bar, 1 μm. (H) TEM micrograph, RCC1997. A terminal valve. Note the central process. Scale bar, 5 μm. (I) TEM micrograph, RCC1997. A girdle band with parallel costae and small poroids. Scale bar, 5 μm. (J-L) *Chaetoceros gelidus*: (J) LM micrograph, RCC2271. A curved chain. Note the two straight setae on the upper part of the picture. Scale bar, 20 μm. (K) LM micrograph, RCC2271. A spherical colony. Scale bar, 50 μm. (L) SEM micrograph, RCC2271. Two intercalary valves with the narrow aperture. Scale bar, 1 μm.

Figure 8. (A-C) *Chaetoceros gelidus*: (A) TEM micrograph, RCC2271. Intercalary valve. Scale bar, 1 μm. (B) SEM micrograph, RCC2271. Detail of the two types of setae, the short (on the upper part of the picture) and the straight long seta (crossing the picture). Note the absence of spines in a large part of the long seta. Scale bar, 5 μm. (C) SEM micrograph, RCC2271. A spore. Scale bar, 1 μm. (D-N) *Chaetoceros neogracilis*: (D) LM micrograph, RCC2272. A solitary cell. Scale bar, 10 μm. (E) LM micrograph, RCC2017. A solitary cell. Scale bar, 10 μm. (F) LM micrograph, RCC2016. A solitary cell. Scale bar, 10 μm. (G) LM micrograph, RCC1989. A colony of four cells. Scale bar, 5 μm. (H) SEM micrograph, RCC2012. Detail of a colony. Note quite narrow apertures. Scale bar, 1 μm. (I) SEM micrograph, RCC2012. Terminal valve with the external tube. Scale bar, 2 μm. (J) TEM micrograph, RCC2012. Terminal valve with the central slit-like process. Scale bar, 2 μm. (K) TEM micrograph, RCC2012. Intercalary valve. Scale bar, 2 μm. (L) TEM micrograph, RCC2271, Intercalary valve. Scale bar, 2 μm. (M) SEM micrograph, RCC2271. Setae with arrowhead-shaped spines. Scale bar, 1 μm. (N) SEM

micrograph, RCC2271. Detail of a seta with spines and long spiral costae interconnected by short transverse costae. Scale bar, 0.5 µm.

Figure 9. Diagrams of the secondary structure of the ITS-2 transcripts of (**A**) *Chaetoceros neogracilis* Clade I RCC2279, (**B**) *Chaetoceros neogracilis* Clade II RCC2318, (**C**) *Chaetoceros neogracilis* Clade III RCC1989, and (**D**) *Chaetoceros neogracilis* Clade IV RCC2010. Base changes between the different genotypes are indicated in red.
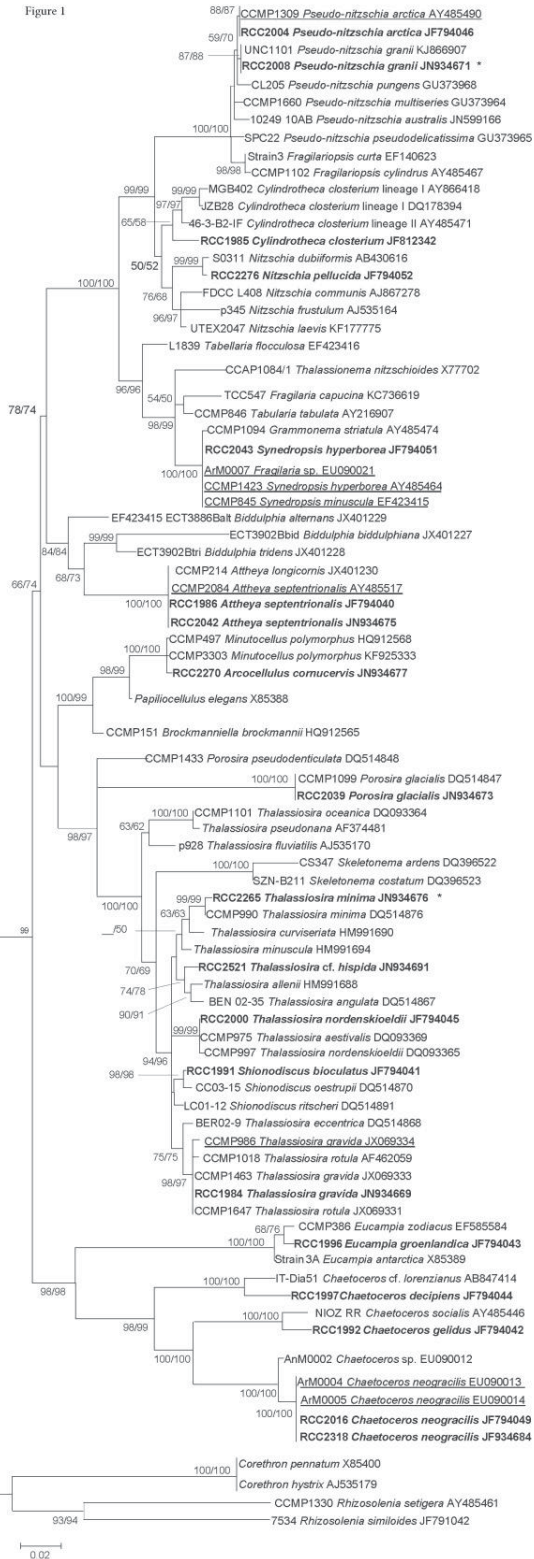
Supporting information

Table S1. Details of the strain isolated during the MALINA cruise and used in the present study. Most strains are available at Roscoff Culture Collection (RCC)

Table S2. List of the strains and species from which the sequences were used in the present study for the phylogenetic trees. Most strains are currently available at different institutions or culture collections. CCMP: National Centre for Marine Algae and Microbiota (ncma.bigelow.org), UNC: Culture Collection at University of North Carolina (www.unc.edu/), NIOZ: Culture Collection at Netherland Institute for Sea Research (www.nioz.nl), UTEX: Culture Collection of Algae at University of Texas Austin (utex.org/), CCAP: Culture Collection of Algae and Protozoa (www.ccap.ac.uk), TCC: Thonon Culture Collection (www6.inra.fr/carrtel-collection_eng), CS: Australia National Algae Culture Collection (www.csiro.au/en/Research/Collections/ANACC/About-our-collection), SZN: Stazione Zoologica Anton Dohrn, Naples (www.szn.it), RCC: Roscoff Culture Collection (http://roscoff-culture-collection.org).

Figure S1. Phylogenetic tree of the ITS operon of the *Chaetoceros* sp. strains isolated in the present study. The Antarctic strains of *Chaetoceros* sp. (CCMP187, CCMP189, CCMP190) were used as outgroup. The bootstrap values are indicated next to the branches as for Figure 6.

Figure 1

Figure 2

Figure 3
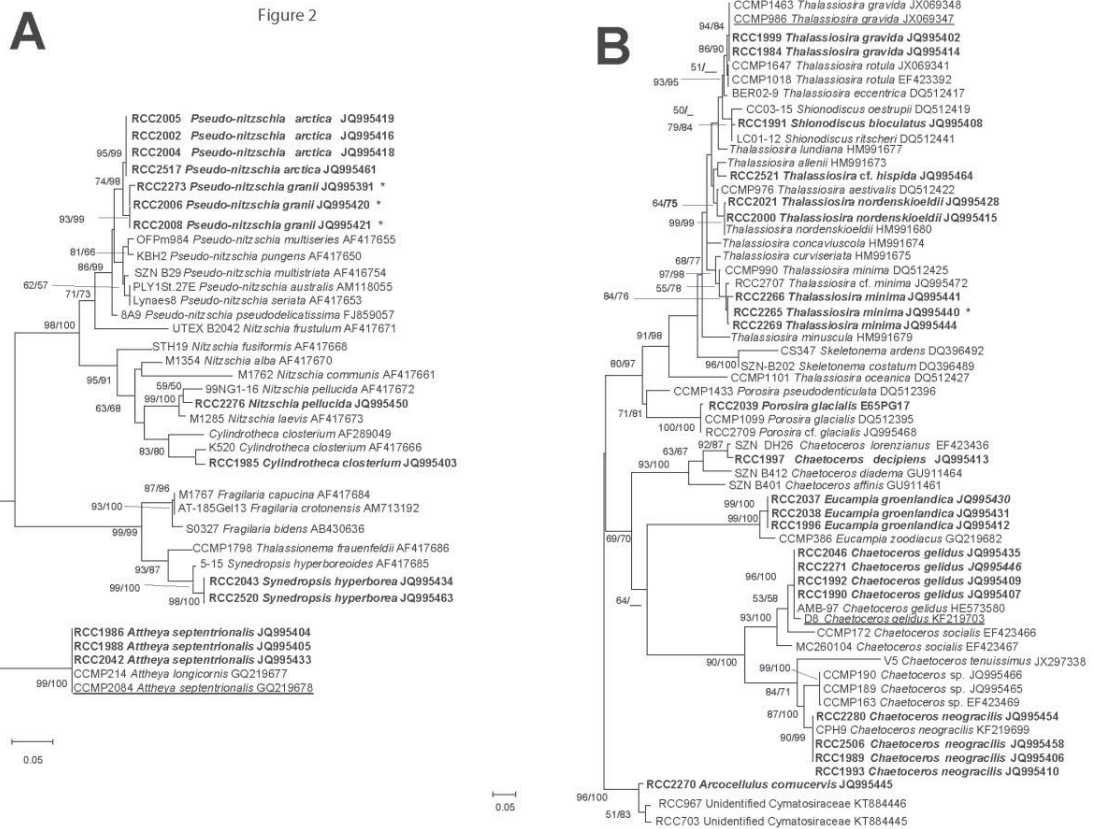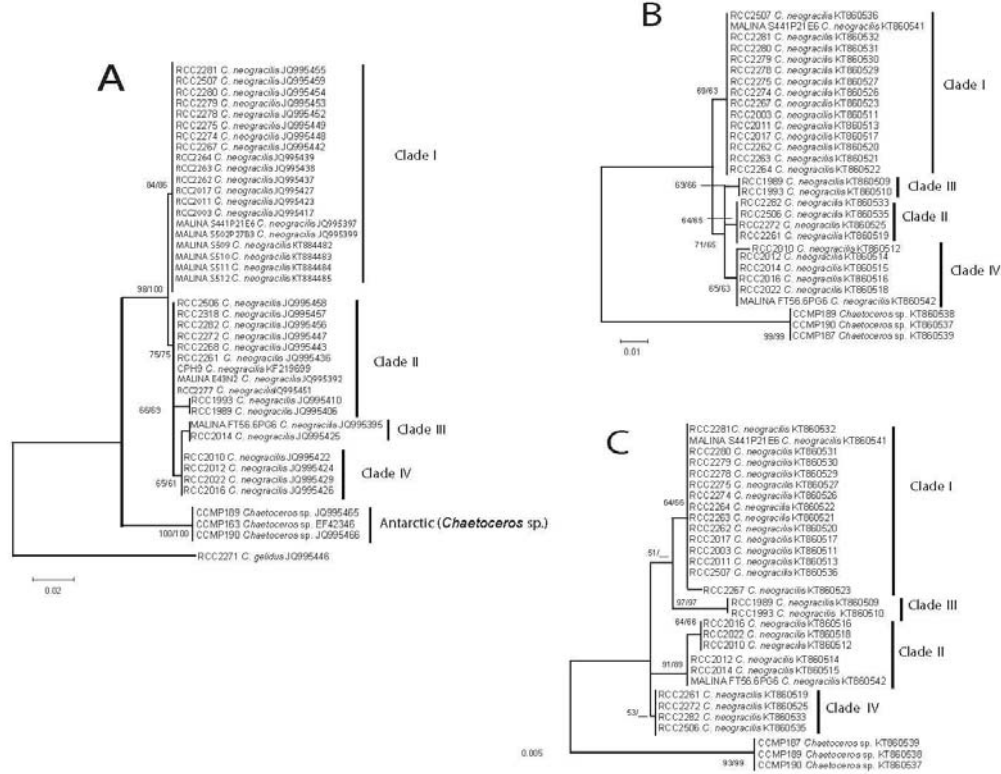
RCC2281 *Chaetoceros neogracilis*
MALINA S441P21E6 *Chaetoceros neogracilis*
RCC2280 *Chaetoceros neogracilis*
RCC2279 *Chaetoceros neogracilis*
RCC2278 *Chaetoceros neogracilis*
RCC2275 *Chaetoceros neogracilis*
RCC2274 *Chaetoceros neogracilis*
44 — RCC2267 *Chaetoceros neogracilis*
RCC2264 *Chaetoceros neogracilis*
RCC2263 *Chaetoceros neogracilis*
45 RCC2262 *Chaetoceros neogracilis*
RCC2017 *Chaetoceros neogracilis*
RCC2011 *Chaetoceros neogracilis*
82 RCC2003 *Chaetoceros neogracilis*
RCC2507 *Chaetoceros neogracilis*
MALINA S502P27B3 *Chaetoceros neogracilis*

Clade I

45

RCC2016 *Chaetoceros neogracilis*
66 RCC2022 *Chaetoceros neogracilis*
RCC2010 *Chaetoceros neogracilis*
RCC2012 *Chaetoceros neogracilis*
97 RCC2014 *Chaetoceros neogracilis*
MALINA FT56.6PG6 *Chaetoceros neogracilis*

Clade IV

49

RCC2261 *Chaetoceros neogracilis*
RCC2268 *Chaetoceros neogracilis*
RCC2272 *Chaetoceros neogracilis*
RCC2277 *Chaetoceros neogracilis*
58 RCC2282 *Chaetoceros neogracilis*
RCC2318 *Chaetoceros neogracilis*
RCC2506 *Chaetoceros neogracilis*

Clade II

RCC1989 *Chaetoceros neogracilis*
99 RCC1993 *Chaetoceros neogracilis*

Clade III

CCMP190 *Chaetoceros* sp.
CCMP189 *Chaetoceros* sp.
100 CCMP187 *Chaetoceros* sp.

Antarctic *Chaetoceros* sp.

5

Supplementary Table S1

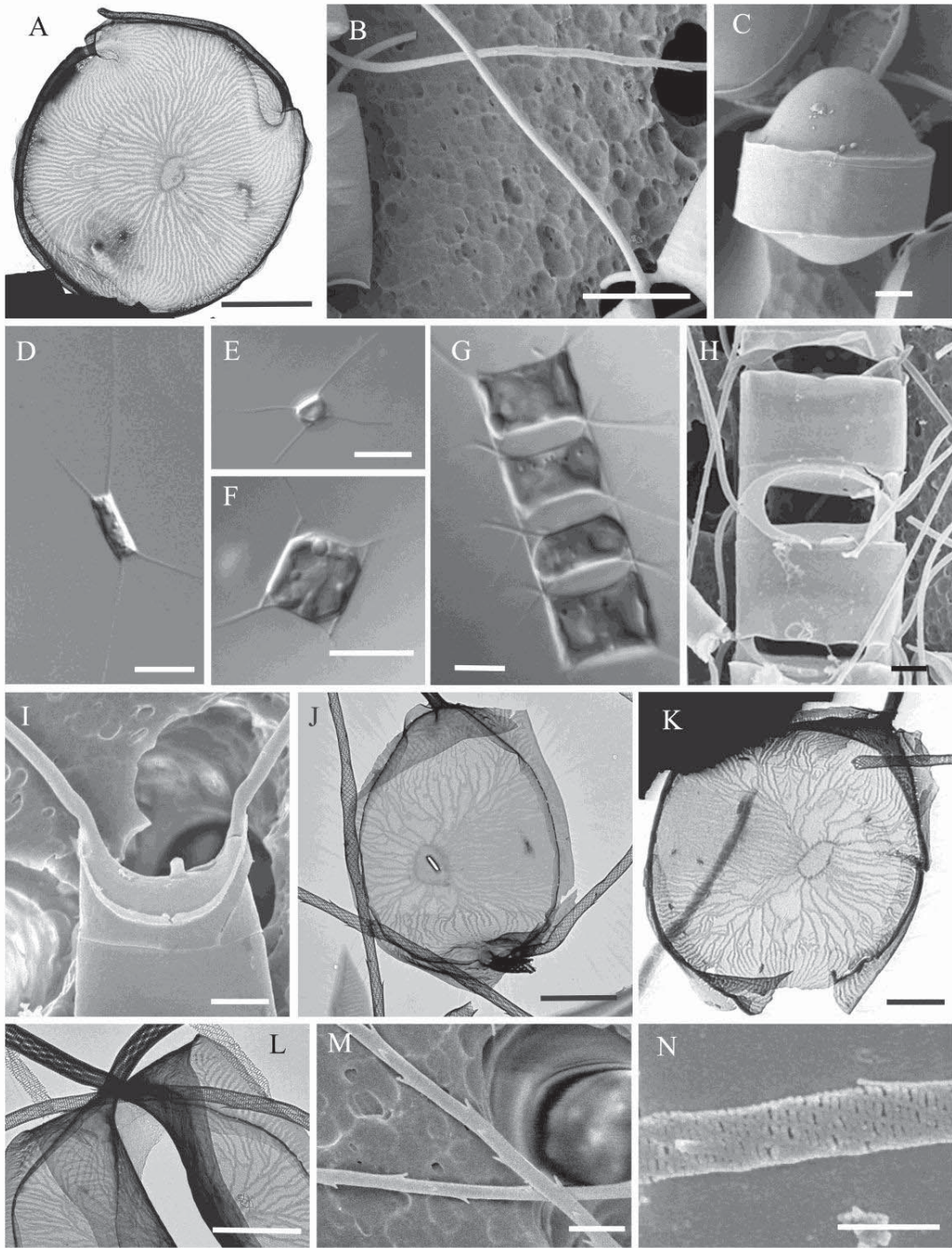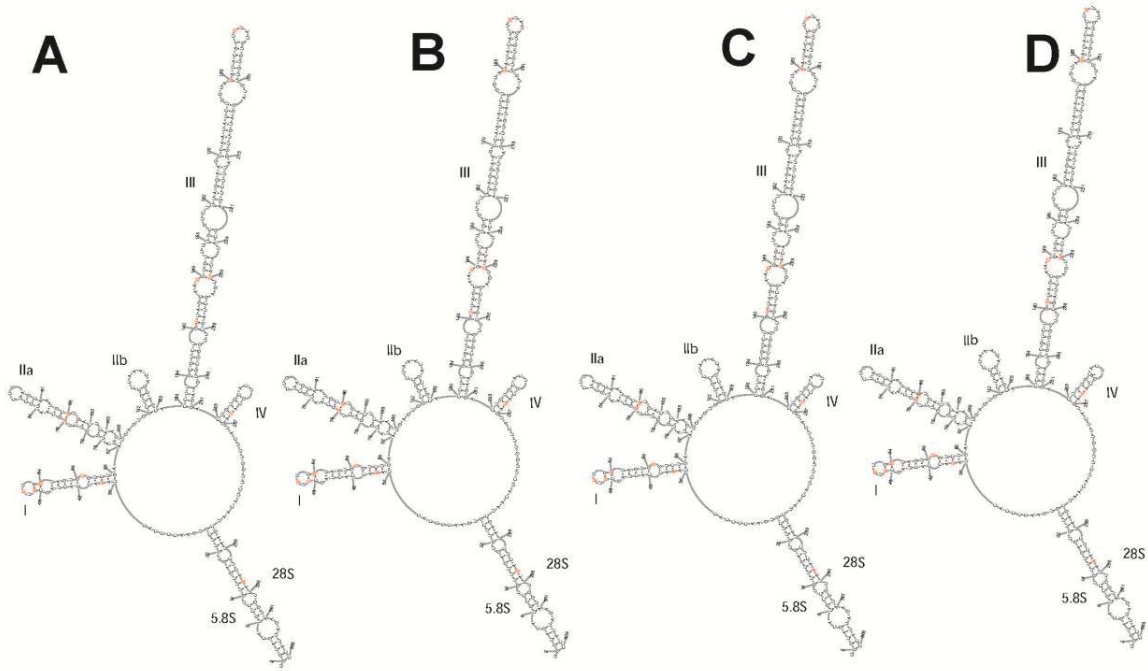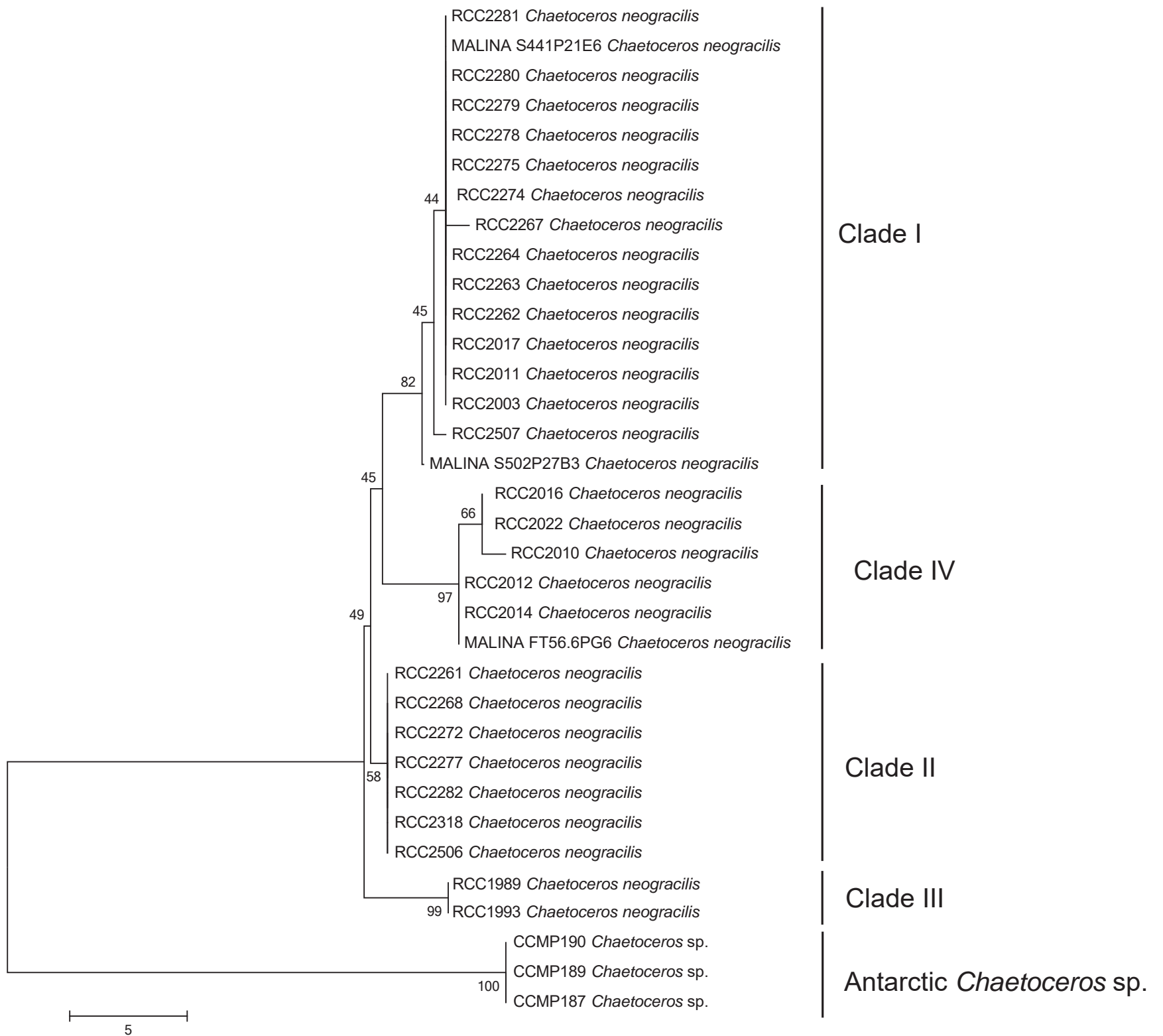| Station	CTD	Depth	Latitude (°N)	Longitude (°W)	Temperature (°C)	Salinity (psu)	Cultures direct FCS[a]	Cultures TFF[b]		Culture Enrichments	
								FCS	Pipette isolation	FCS	Pipette isolation
PAC05		3								1	
PAC06		3	50.06	-139.53	12.1	32.5				1	
PAC08		3	53.36	159.29	11.8	32.7					2
ARC12		3	71.19	159.42	2	30.5	1				
BEA13		3	70.56	145.4	8.8	17.6	2			2	
BEA14		3	70.5	135.5	3.3	25.6	1			1	
110	56	3	71.7	-126.48	4.4	28.7			3		
235	191	3	71.76	-130.83	0	27.3		3			
235	191	25	71.76	-130.83	1.6	29.9		1			
280	42	30	70.87	-130.51	-0.7	32.2			8		
320	82	3	71.57	-133.94	-0.8	27		3			
394	38	3	69.85	-133.49	7	25.1	3				
460	145	3	70.68	-136.05			2				
620	99	3	70.68	-139.63	1.6	22.1		2	3		
620	99	65	70.68	-139.63	-1.1	30.7		1	5		
680	35	3	69.6	-138.23	8.3	14.7			3		
680	35	40	69.6	-138.23	-1.2	31.3		1			
690	31	3	69.49	-137.94	7.4	19	1				
690	31	29	69.49	-137.94	-1.3	31.2					16
760	106	3	70.55	-140.8	0.6	22.3		8	2		
Total							10	19	24	5	18

Supplementary Table S2

Strain ID	Strain name	Authors	Geographical origin	Genbank 18S	Genbank 28S	Genbank ITS
CCMP214	*Attheya longicornis*	Crawford & Gardner	Gulf of Maine, North Atlantic Ocean	JX401230	GQ219677	
CCMP2084	*Attheya septentrionalis*	(Østrup) Crawford	Baffin Bay, Arctic	AY485517	GQ219678	
ECT3886Balt	*Biddulphia alternans*	(Bailey) Van Heurck	Kahana Bay, North Pacific Ocean	JX401229		
ECT3902Bbid	*Biddulphia biddulphiana*	(J.E.Smith) Boyer	Unknown	JX401227		
ECT3902 Btri	*Biddulphia tridens*	(Ehrenberg) Ehrenberg	Long Beach, North Pacific Ocean	JX401228		
CCMP151	*Brockmanniella brockmanni*	(Hustedt) Hasle, Stosch & Syvertsen	Unknown	HQ912565		
SZN B401	*Chaetoceros affinis*	Lauder	Unknown		GU911461	
SZN-B412	*Chaetoceros diadema*	(Ehrenberg) Gran	Gulf of Naples, Mediterranean Sea		GU911464	
AMB-97	*Chaetoceros gelidus*	Chamnansinp, Li, Lundholm & Moestrup	Tromso, North Atlantic Ocean		HE573580	
D8	*Chaetoceros gelidus*	Chamnansinp, Li, Lundholm & Moestrup	Kattegat Bay, North Sea		KF219703	
SZN-DH26	*Chaetoceros lorenzianus*	Grunow	Gulf of Naples, Mediterranean Sea		EF423436	
IT-Dia51	*Chaetoceros cf. lorenzianus*	Grunow	Aki nada Sea, Indian Ocean	AB847414		
ArM0004	*Chaetoceros neogracilis*	(Schütt) VanLandingham	Svalbard, Arctic Ocean	EU090013		
ArM0005	*Chaetoceros neogracilis*	(Schütt) VanLandingham	Svalbard, Arctic Ocean	EU090014		
CPH9	*Chaetoceros neogracilis*	(Schütt) VanLandingham	Hellerup Harbour, Baltic Sea		KF219699	
CCMP172	*Chaetoceros socialis*	Lauder	Friday Harbour, North Pacific Ocean		EF423466	
MC260104	*Chaetoceros socialis*	Lauder	Gulf of Naples, Mediterranean Sea		EF423467	
NIOZ RR	*Chaetoceros socialis*	Lauder	Unknown	AY485446		
AnM0002	*Chaetoceros* sp.		King George Island, Antarctica	EU090012		
CCMP163	*Chaetoceros* sp.		Southern Ocean		EF426369	
CCMP187	*Chaetoceros* sp.		Weddell Sea, Antarctica			KT860539
CCMP189	*Chaetoceros* sp.		Weddell Sea, Antarctica		JQ995466	KT860538
CCMP190	*Chaetoceros* sp.		Weddell Sea, Antarctica		JQ995465	KT860537
V5	*Chaetoceros tenuissimus*	Meunier	Black Sea		JX297338	
Unavailable	*Corethron pennatum*	(Grunow) Ostenfeld	Unknown	X85400		
Unavailable	*Corethron hystrix*	Hensen	Unknown	AJ535179		
MGB402	*Cylindrotheca closterium*	(Ehrenberg) Lewin & Reimann	Qindao Bay, Indian Ocean	AY866418		
JZB28	*Cylindrotheca closterium*	(Ehrenberg) Lewin & Reimann	Qindao Bay, Indian Ocean	DQ178394		
NIOZ (46-3-B2-IF)	*Cylindrotheca closterium*	(Ehrenberg) Lewin & Reimann	Unknown	AY485471		
K520	*Cylindrotheca closterium*	(Ehrenberg) Lewin & Reimann	Kattegat Bay, North Sea		AF417666	
Unavailable	*Cylindrotheca closterium*	(Ehrenberg) Lewin & Reimann	Unknown		AF289049	
Strain 3A	*Eucampia antarctica*	(Castracane) Mangin	Unknown	X85389		
CCMP386	*Eucampia zodiacus*	Ehrenberg	Gulf of Maine, North Atlantic Ocean	EF585584	GQ219682	
S0327	*Fragilaria bidens*	Heiberg	Unknown		AB430636	
TCC547	*Fragilaria capucina*	Desmazières	Unknown	KC736619		
M1767	*Fragilaria capucina*	Desmazières	Cologne pond, Germany		AF417684	
AT-185Gel3	*Fragilaria crotonensis*	Kitton	Bremen pond, Germany		AM713192	
AnM0007	*Fragilaria* sp.		Svalbard, Arctic Ocean	EU090021		
Strain 3	*Fragilariopsis curta*	(Van Heurck) Hustedt	Mertz glacier, Antarctica	EF140623		
CCMP1102	*Fragilariopsis cylindrus*	(Grunow) Helmcke & Krieger	Islas Orcadas, Antarctica	AY485467		
CCMP1094	*Grammonema striatula*	C.Agardh	Gulf of Alaska, North Pacific Ocean	AY485474		
CCMP497	*Minutocellus polymorphus*	(Hargraves & Guillard) Hasle, Stosch, & Syv	Bermuda, North Atlantic Ocean	HQ912568		
CCMP3303	*Minutocellus polymorphus*	(Hargraves & Guillard) Hasle, Stosch, & Syv	Angola coast, South Atlantic Ocean	KF925333		
M1354	*Nitzschia alba*	J.C.Lewin & R.A.Lewin	Roscoff, English Channel		AF417670	
M1762	*Nitzschia communis*	Rabenhorst	Cologne Botanical Garden, Germany		AF417661	
FDCC L408	*Nitzschia communis*	Rabenhorst	Unknown	AJ867278		
S0311	*Nitzschia dubiformis*	Hustedt	Unknown	AB430616		
STH19	*Nitzschia fusiformis*	Grunow	Isefjord, Kattegat Bay, North Sea		AF417668	
p345	*Nitzschia frustulum*	(Kützing) Grunow	Unknown	AJ535164		
UTEXB2042	*Nitzschia frustulum*	(Kützing) Grunow	la Jolla, California, North Atlantic Ocean		AF417671	
UTEX2047	*Nitzschia laevis*	Hustedt	Woods Hole, North Atlantic Ocean	KF177775		
M1285	*Nitzschia laevis*	Hustedt	Dusseldorf pond, Germany		AF417673	
99NG1-16	*Nitzschia pellucida*	Grunow	Ishigaki Island, Japan		AF417672	
Unavailable	*Papiliocellulus elegans*	Hasle, Stosch & Syvertsen	Unknown	X85388		
CCMP1099	*Porosira glacialis*	(Grunow) Jørgensen	Islas Orcadas, Antarctica	DQ514847	DQ512395	
RCC2709	*Porosira cf. glacialis*	(Grunow) Jørgensen	Fildes Bay, Antarctica		JQ995468	
CCMP1433	*Porosira pseudodenticulata*	(Hustedt) Jousé	Ross Sea, Antarctica	DQ514848	DQ512396	
CCMP1309	*Pseudo-nitzschia arctica*	Percopo & Sarno	Barrow Strait, Canada	AY485490		
10249 10AB	*Pseudo-nitzschia australis*	Frenguelli	Monterey Bay, North Pacific Ocean	JN599166		
Ply1St.27E	*Pseudo-nitzschia australis*	Frenguelli	Loch Lihne, North Atlantic Ocean		AM118055	
UNC1101	*Pseudo-nitzschia granii*	(Hasle) Hasle	Gulf of Alaska, North Pacific Ocean	KJ866907		
CCMP1660	*Pseudo-nitzschia multiseries*	(Hasle) Hasle	Gulf St Lawrence, North Atlantic Ocean	GU373964		
OFPm984	*Pseudo-nitzschia multiseries*	(Hasle) Hasle	Ofunato Bay, Indian Ocean		AF417655	
SZNB29	*Pseudo-nitzschia multistriata*	(Takano) Takano	Gulf of Naples, Mediterranean Sea		AF416754	
SPC22	*Pseudo-nitzschia pseudodelicatissima*	(Hasle) Hasle	San Pedro Channel, North Pacific Ocean	GU373965		
8A9	*Pseudo-nitzschia pseudodelicatissima*	(Hasle) Hasle	Thermaikos Gulf, Mediterranean Sea		FJ859057	
CL205	*Pseudo-nitzschia pungens*	(Grunow ex Cleve) Hasle	Lennox Channel, North Atlantic Ocean	GU373968		
KBH2	*Pseudo-nitzschia pungens*	(Grunow ex Cleve) Hasle	Khan Hoa Bay, Indian Ocean		AF417650	
Linaes8	*Pseudo-nitzschia seriata*	(Cleve) H.Peragallo	Isefjord, Kattegat Bay, North Sea		AF417653	
CCMP1440	*Pseudo-nitzschia* sp.		McMurdo Sound, Antarctica	GU373969		
CCMP1330	*Rhizosolenia setigera*	Brightwell	Massacchussets, USA	AY485461		
7534	*Rhizosolenia similoides*	Cleve	Gulf of Mexico, North Atlantic Ocean	JF791042		
CC03-15	*Shionodiscus oestrupii*	(Ostenfeld) Alverson, Kang & Theriot	Sargassum Sea, North Atlantic Ocean	DQ514870	DQ512419	
LC01-12	*Shionodiscus ritscheri*	(Hustedt) Alverson, Kang & Theriot	Drake Passage, Southern Ocean	DQ514891	DQ512441	
CS347	*Skeletonema ardens*	Sarno & Zingone	Gulf of Carpentaria, Indian Ocean	DQ396522	DQ396492	
SZN-B202	*Skeletonema costatum*	(Greville) Cleve	Indian River Lagoon, FL, USA		DQ396489	
SZN B211	*Skeletonema costatum*	(Greville) Cleve	Montevideo coast, South Atlantic Ocean	DQ396523		
CCMP1423	*Synedropsis hyperborea*	(Grunow) Hasle, Medlin & Syvertsen	Baffin Bay, Arctic	AY485464		
5-15	*Synedropsis hyperboreoides*	Hasle, Medlin & Syvertsen	Ross Sea, Antarctica		AF417685	
CCMP845	*Synedropsis minuscula*	(Grunow) Kooistra	Baffin Bay, Arctic	EF423415		
L1839	*Tabellaria flocculosa*	(Roth) Kützing	Unknown	EF423416		
CCMP846	*Tabularia tabulata*	(Agardh) Snoeijs	Gulf of Alaska, North Pacific Ocean	AY216907		
CCMP1798	*Thalassionema frauenfeldii*	(Grunow) Tempère & Peragallo	North Atlantic Ocean		AF417686	
CCAP1084/1	*Thalassionema nitzschioides*	(Grunow) Mereschkowsky	Unknown	X77702		
CCMP975	*Thalassiosira aestivalis*	Gran	Gulf of Maine, North Atlantic Ocean	DQ093369		
CCMP975	*Thalassiosira aestivalis*	Gran	Vancouver coast, North Pacific Ocean		DQ512422	
Unknown	*Thalassiosira allenii*	Takano	Unknown	HM991688	HM991673	
BEN 02-35	*Thalassiosira angulata*	(Gregory) Hasle	San Joaquin River, California, USA	DQ514867		
Unavailable	*Thalassiosira concaviuscola*	Makarova	Unknown		HM991674	
Unavailable	*Thalassiosira curviseriata*	Takano	Unknown	HM991690	HM991675	
BER02-9	*Thalassiosira eccentrica*	(Ehrenberg) Cleve	San Francisco Bay, North Pacific Ocean	DQ514868	DQ512417	
p928	*Thalassiosira fluviatilis*	Hustedt	Unknown	AJ535170		
CCMP986	*Thalassiosira gravida*	Cleve	Tromso, North Atlantic Ocean	JX069334	JX069347	
CCMP1463	*Thalassiosira gravida*	Cleve	McMurdo Sound, Antarctica	JX069333	JX069348	
Unknown	*Thalassiosira lundiana*	Fryxell	Unknown		HM991677	
CCMP990	*Thalassiosira minima*	Gaarder	Unknown	DQ514876	DQ512425	
RCC2707	*Thalassiosira cf. minima*	Gaarder	Fildes Bay, Antarctica		JQ995472	
Unavailable	*Thalassiosira minuscula*	Krasske	Unknown	HM991694	HM991679	
CCMP997	*Thalassiosira nordenskioeldii*	Cleve	Norwegian Sea, North Atlantic Ocean	DQ093365		
Unavailable	*Thalassiosira nordenskioeldii*	Cleve	Unknown		HM991680	
CCMP1101	*Thalassiosira oceanica*	Hasle	Islas Orcadas, Antarctica	DQ093364	DQ512427	
Unavailable	*Thalassiosira pseudonana*	Hasle & Heimdal	Unknown	AF374481		
CCMP1018	*Thalassiosira rotula*	Meunier	California Bight, North Pacific Ocean	AF462059	EF423392	
CCMP1647	*Thalassiosira rotula*	Meunier	Gulf of Naples, Mediterranean Sea	JX069331	JX069341	
RCC967	Unidentified Cymatosiraceae		Chile upwelling, South Pacific Ocean		KT884446	
RCC703	Unidentified Cymatosiraceae		South Africa Coast		KT884445	